JAMES | Journal of Advances in Modeling Earth Systems

RESEARCH ARTICLE
10.1029/2023MS003736

Non-Uniqueness in ITCZ Latitude Due To Radiation-Circulation Coupling in an Idealized GCM

Pablo Zurita-Gotor[1,2], Isaac M. Held[3], Timothy M. Merlis[3], Chiung-Yin Chang[3], Spencer A. Hill[3,4], and Cameron G. MacDonald[3]

[1]Dpto. Física de la Tierra y Astrofísica, Universidad Complutense de Madrid, Madrid, Spain, [2]Instituto de Geociencias (IGEO) UCM-CSIC, Madrid, Spain, [3]Program in Atmospheric and Oceanic Sciences, Princeton University, Princeton, NJ, USA, [4]Lamont-Doherty Earth Observatory, Columbia University, Palisades, NY, USA

Key Points:

- The equatorial ITCZ can be destabilized by radiation-circulation coupling in a hemispherically symmetric aquaplanet model
- As the ITCZ drifts off the equator two different asymmetric equilibria may exist under symmetric forcing and boundary conditions
- A theory is proposed based on the energy flux equator sensitivity to the perturbed asymmetric heating when the ITCZ moves off the equator

Correspondence to:
P. Zurita-Gotor,
pzurita@alum.mit.edu

Citation:
Zurita-Gotor, P., Held, I. M., Merlis, T. M., Chang, C.-Y., Hill, S. A., & MacDonald, C. G. (2023). Non-uniqueness in ITCZ latitude due to radiation-circulation coupling in an idealized GCM. *Journal of Advances in Modeling Earth Systems*, *15*, e2023MS003736. https://doi.org/10.1029/2023MS003736

Received 30 MAR 2023
Accepted 8 SEP 2023

Abstract An idealized aquaplanet moist global atmospheric model with realistic radiative transfer but no clouds and no convective parameterization is found to possess multiple climate equilibria. When forced symmetrically about the equator, in some cases the Inter Tropical Convergence Zone (ITCZ) migrates to an off-equatorial equilibrium position. Mechanism denial experiments prescribing relative humidity imply that radiation-circulation coupling is essential to this instability. The cross-equatorial asymmetry occurs only when the underlying slab ocean is sufficiently deep and the atmosphere's spectral dynamical core is sufficiently coarse (~T170 or less with our control parameters). At higher resolutions, initializing with an asymmetric state indicates metastability with very slow (thousands of days) return to hemispheric symmetry. There is some sensitivity to the model timestep, which affects the time required to transition to the asymmetric state, with little effect on the equilibrium climate. The instability is enhanced when the planetary boundary layer scheme favors deeper layers or by a prescribed meridional heat transport away from the equator within the slab. The instability is not present when the model is run with a convective parameterization scheme commonly utilized in idealized moist models. We argue that the instability occurs when the asymmetric heating associated with a spontaneous ITCZ shift drives a circulation that rises poleward of the perturbed ITCZ. These results serve as a warning of the potential for instability and non-uniqueness of climate that may complicate studies with idealized models of the tropical response to perturbations in forcing.

Plain Language Summary Much of the rainfall in the tropics occurs in the Intertropical Convergence Zones (ITCZs). These regions are associated with the convergence of surface winds, which produces the rising air required to feed the Hadley cells. The ITCZ location is known to be determined by the spatial distribution of atmospheric heating as the Hadley cells act to erase thermal imbalance within the tropics. With hemispherically symmetric heating, a symmetric equatorial ITCZ is expected. However, it is shown in this paper that changes in the ITCZ location affect the distribution of the radiative cooling of the atmosphere through changes in the water vapor distribution, which may make the equatorial ITCZ unstable under some circumstances. In this situation, two alternative climates with the ITCZ shifted into either one of the hemispheres exist. This instability may play an important role for understanding the distribution of tropical precipitation and the potential for the existence of multiple climates for the same set of external conditions.

1. Introduction

In climate models, the typically smooth behavior of the climate as a function of parameters or external forcing can potentially be altered dramatically by sharp bifurcations and non-uniqueness. Examples typically involve interactions between the atmosphere and the oceans, land, or ice (e.g., Atlantic Meridional Overturning Circulation shut-off (Manabe & Stouffer, 1988), vegetation feedbacks maintaining the Green Sahara (Hopcroft et al., 2021), and Snowball Earth instability (Voigt & Marotzke, 2010)). Examples involving only the atmosphere in any significant way are rarer, despite the potential for complexity given the atmosphere's turbulent and chaotic flow. Here, we present an example of non-uniqueness in a class of idealized atmospheric general circulation models (GCMs) arising from spontaneous breaking of climate symmetry about the equator, associated with the Intertropical Convergence Zone (ITCZ) migrating off the equator into one hemisphere under hemispherically symmetric boundary conditions. When this "ITCZ instability" occurs there are two equilibria, one with the ITCZ north and the other south of the equator.

There is an extensive literature on idealized atmospheric GCMs with zonally symmetric boundary conditions. Here, we are focused on models with active hydrological cycles, where the phase change of water vapor affects the atmospheric flow through latent heating. In one popular class of idealized models with active hydrological cycles the radiation is decoupled from the water cycle by using gray radiation (Frierson et al., 2006), which is only a function of temperature and pressure (Goody & Yung, 1995). One can motivate this choice by the conceptual simplicity of separating off the uncertain role of radiative processes to focus on the interaction between latent heat release and the atmospheric circulation. However, there has been an increasing amount of research on idealized GCMs that use comprehensive radiative transfer, retaining in particular the robust clear-sky water vapor effects on radiation, while discarding the more model-dependent cloud radiative effects (Clark et al., 2018; Jucker & Gerber, 2017; MacDonald & Ming, 2022; Merlis et al., 2013a). It is this class of idealized GCMs that we examine here. This configuration allows for radiation-circulation feedbacks, in which changes in the circulation impact atmospheric heating by modulating the relative humidity distribution. As the tropical heating distribution constrains the ITCZ position and structure (Adam, 2021; Bischoff & Schneider, 2014; Kang et al., 2008; Lindzen & Hou, 1988; Schneider et al., 2014), it will be shown in this paper that this feedback loop can make the equatorial ITCZ unstable in some cases. Other studies exposing the complexity introduced by the same set of interactions include bifurcations in single column models (e.g., Raymond & Zeng, 2000; Sobel et al., 2007) and models of spontaneous Hadley cells (e.g., Barsugli et al., 2005; Kirtman & Schneider, 2000; Raymond, 2000), in addition to the extensive literature on spontaneous aggregation in radiative -convective equilibrium (see Wing et al. (2017) for a review).

The other choice that we have made in this study is to focus primarily on models with no closure schemes for either deep or shallow convection. We refer to this setup as large-scale condensation-only (LSC). This choice is consistent with the goal of creating a relatively robust point of comparison for similar studies probing the sensitivity of the results to the choice of convection scheme. Many papers using idealized moist GCMs have used the same simple Betts-Miller scheme described in Frierson (2007b) that relaxes unstable columns to moist adiabats when there is adequate water to produce a specified relative humidity. Some studies examine the effects of varying parameters in that scheme (Frierson, 2007a; Merlis & Schneider, 2011). But it is still not well understood which features of convective closures control large-scale dynamical responses across classes of convection schemes of interest more generally. The LSC model can be thought of a natural starting point for such studies. Existing research that has used idealized moist GCMs without convection schemes include Frierson et al. (2006), Rios-Berrios et al. (2022), and Labonté and Merlis (2023).

The work of Clark et al. (2018) has provided motivation for this study. Using a setup very similar to that utilized in this paper (a moist aquaplanet with realistic clear sky radiative transfer) but with the convection scheme of Frierson (2007b), they study how the response of the ITCZ to an imposed cross-equatorial heat flux is modified by water vapor feedback. Although not discussed in that paper, the same model but with the convection scheme turned off results in the ITCZ instability described here, with an asymmetric circulation even in the absence of the imposed cross-equatorial heat flux. Zhihong Tan (personal communication) has also encountered this instability when running a GCM with a similar set of idealizations (slab aquaplanet with realistic clear-sky radiation, but with an eddy-diffusivity/mass-flux parameterization for the boundary layer and convection).

Using a standard spectral dynamical core, we vary the resolution from T42 to T255 (meridional grid spacing in the transform grid of roughly 300 to 50 km). We do not try to push our resolution to nonhydrostatic scales. Given the variety of sensitivities of this ITCZ instability to parameters and external forcing in the simulations described below, our view is that we need to explore these sensitivities at the modest resolution typical of current Coupled Model Intercomparison Project (CMIP) climate models and idealized GCMs. We can then determine which, if any, configurations would be most valuably studied at much higher resolution.

We run the model with a slab ocean lower boundary condition so that the model is energetically closed except for the top-of-atmosphere (TOA) radiative fluxes. We find that the heat capacity of this slab must exceed a critical value, comparable to the heat capacity of the atmosphere, for this ITCZ instability to exist. We also find sensitivity to the depth of the planetary boundary layer and to the prescription of "oceanic" poleward energy transport within the slab. The double-ITCZ state that can be created with imposed slab poleward energy transport in other idealized models (Bischoff & Schneider, 2016) is inhibited when parameters are such that the cross-equatorial instability is present.

We describe the idealized GCM and parameters that we vary in Section 2. Section 3 introduces the ITCZ instability in a control simulation. It also contains results from simulations in which we manipulate the climatological relative humidity distribution to help make the case that the modification of this distribution is a key to

this instability. Section 4 surveys the sensitivities of the instability to resolution and model configuration while Section 5 describes results with an idealized convection scheme. Section 6 provides a simplified conceptual framework for the instability that helps rationalize the sensitivities uncovered in the GCM qualitatively. We conclude with a summary of the main results in Section 7.

2. Model Description

We use in this study an idealized moist GCM extracted from the Isca (Vallis et al., 2018) code base (commit 9560521e1ba5ce27a13786ffdcb16578d0bd00da) maintained at the University of Exeter, building on the Flexible Modeling System and the spectral dynamics code originally developed at the Geophysical Fluid Dynamics Laboratory of the National Oceanic and Atmospheric Administration. The model incorporates a simplified hydrological cycle in the spirit of Frierson et al. (2006) that includes water vapor advection and liquid-vapor phase change but no clouds. All the condensate is rained out immediately in this standard setup, but we also test the consequences of an alternative setting in which reevaporation is required to saturate all layers below the level of condensation before rain is allowed to reach the surface, providing the maximum increase in relative humidity that reevaporation can provide (this is achieved by setting *do_evap* to true in the lscale_cond_nml namelist). The specific humidity is a grid variable advected with a finite-volume scheme and is not spectrally transformed. The model is run with no convective parameterization, using large-scale condensation (LSC) only, except for a few simulations described in Section 5 using the simplified Betts-Miller (SBM) scheme of Frierson (2007b) for comparison.

A key difference from Frierson et al. (2006) is the use of full instead of gray radiation following previous studies (Jucker & Gerber, 2017; Merlis et al., 2013a). Radiative transfer is computed using the RRTMG model (Mlawer et al., 1997). We set the obliquity and eccentricity to zero to eliminate the seasonal cycle but keep the diurnal cycle, avoiding the need for defining an effective diurnally averaged zenith angle. The CO_2 concentration is 300 ppmv, there are no other well-mixed greenhouse gases, and there is no ozone. The solar constant is 1,365 W m^{-2}. We use a surface albedo value of 0.22 to produce Earth-like tropical surface temperatures given the absence of clouds and a relatively dry troposphere.

The model is run over a slab ocean with no heat transport within the slab (i.e., no ocean Q-fluxes) by default. We use a control depth of 20 m but this value is changed in some experiments, including a "swamp" limit with zero heat capacity. We utilize the option of computing the planetary boundary layer (PBL) depth with a critical bulk Richardson number (Ri_c) between the surface and the top of the PBL, as described in Frierson et al. (2006), but here we use this scheme in both stable and unstable PBL conditions to provide a simple way of modifying the PBL depth through the value of Ri_c. This PBL formulation is obtained by setting *do_simple* to true in the diffusivity_nml namelist. We use the full Monin-Obukhov similarity theory in both stable and unstable conditions, with the similarity functions and the roughness formulation maintained at the default settings in the code.

Except when otherwise indicated above, our control configuration is based on Isca's default template for the "MiMA" case of Jucker and Gerber (2017). We run the spectral core over a range of horizontal resolutions (T42 to T255) to probe the resolution dependence of the instability. We use 30 unequally spaced sigma levels, with a near-surface resolution of 20 hPa and a model top at 4 hPa. Motivated by the study of Williamson and Olson (2003), who describes a timestep dependence of the ITCZ structure in an aquaplanet model with cloud-radiative interactions and convective parameterization, we also explore the sensitivity to timestep at fixed resolution. But our focus on sensitivity to numerics is preliminary; in particular, we have not examined the dependence on vertical resolution or alternative dynamical cores.

3. A Hemispherically Asymmetric Climate

A model with T85 horizontal resolution, 20 m depth slab ocean and no convective closure is chosen as the control from which we then modify resolution and parameters. Figure 1 shows the evolution of the zonal-mean precipitation over 5,000 days in this simulation, initialized from an isothermal state of rest plus noise. The model ITCZ initially forms at the equator and shows some preference for off-equatorial precipitation in alternating hemispheres after day 1,200, but then definitively moves into one hemisphere after about 2,000 days. The averaged zonal-mean precipitation over the last 2,500 days of the simulation is shown in Figure 2a. A single ITCZ is located at 8° latitude in the Northern Hemisphere, co-located with the maximum slab temperature.

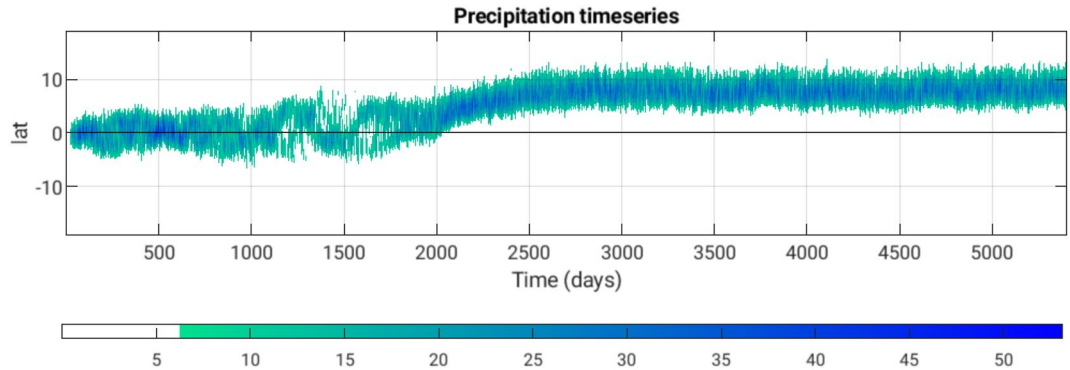

Figure 1. Time series of zonal-mean precipitation (mm/day) for a T85 simulation with no convective parameterization and a 20 m deep slab ocean.

The underlying numerical model, the incident solar flux, and boundary conditions are all symmetric about the equator. If we take the final state (at day 5,400) from this control run, reflect this state across the equator and use it to initialize a new simulation the ITCZ is then maintained in the Southern Hemisphere. Therefore, the model's climate is not unique—the ITCZ would be confined to the Southern Hemisphere for a different choice of random perturbation to the same symmetric initial conditions.

The other panels in Figure 2 show the time- and zonal-mean meridional circulation, relative humidity, outgoing longwave radiation at the top of the atmosphere (OLR) and net column heating. These emphasize the strong cross-equatorial asymmetry in the model climate. In particular, the strengths of the Hadley cells in the two hemispheres differ by a factor of 2.7. Albeit weaker than in solstitial conditions on Earth (for which values of 4–6 for this ratio are typical), the degree of asymmetry is remarkable given the symmetric setup.

Given the absence of clouds in this model, the bulk of the asymmetry in the OLR is a consequence of the asymmetry of the relative humidity, with the minimum in the OLR co-located with the maximum relative humidity

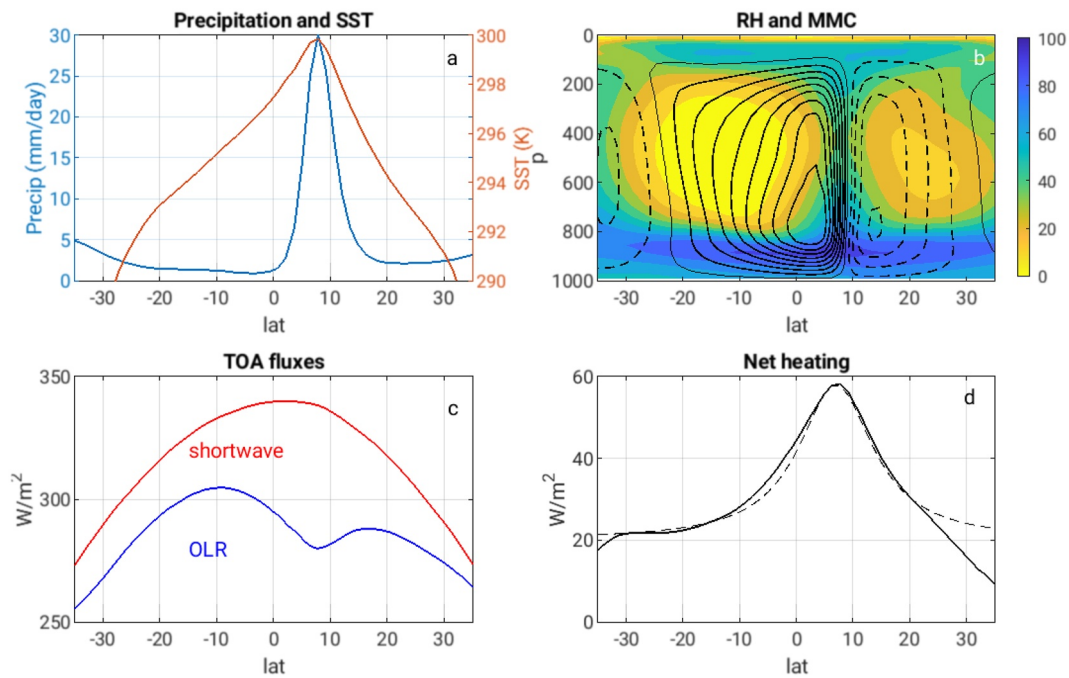

Figure 2. The climatology of the equilibrated control T85 simulation: (a) Time- and zonal-mean precipitation and SST; (b) Zonal-mean relative humidity (shading, contour interval 10%) and mean meridional circulation (contours every 50 Sv starting at ±25 Sv); (c) Top of the atmosphere net shortwave flux (red) and outgoing longwave radiation (blue); (d) Net column heating (solid) and Lorentzian fit (Equation 1, dashed).

at the displaced ITCZ. (The effect of surface temperature on OLR is smaller and would in isolation result in the opposite sign of OLR asymmetry across the equator.) The ITCZ OLR is ∼8 W m^{-2} smaller than the subtropical OLR maxima in the same hemisphere and ∼25 W m^{-2} in the opposite hemisphere. For reference, the corresponding observed OLR dip based on annual-mean CERES-EBAF data (Loeb et al., 2018) is about 10 W m^{-2} in clear-sky conditions and 32 W m^{-2} for all-sky (22 W m^{-2} using hemispherically symmetrized data).

Given that there is no time-averaged heat flux into the lower boundary, and that the effect of water vapor in the shortwave is relatively small, the latitudinal distribution of the vertically integrated heating of the atmosphere is determined by the asymmetric OLR, which implies that the water vapor radiative feedback is key to this instability. Consistently, simulations using gray radiation, following Frierson et al. (2006), with the same setup as our control simulation otherwise, produce an equatorially symmetric climate. In the substantial literature describing simulations with this gray model, we are aware of no discussion of spontaneously asymmetric climates of the sort described here, though Bellon and Sobel (2010) provides an example of multiple/asymmetric equilibria in the absence of radiative feedbacks in a simplified model.

3.1. Impact of RH Structure

We have found it useful for understanding the impact of the relative humidity (RH) asymmetry to manipulate these simulations by prescribing the RH field seen by the radiation to distributions obtained by perturbing the climatological RH of the control run. In all these simulations the RH used for the radiation computation is prescribed over the interior tropical troposphere (150–850 hPa, 30°S–30°N), with the full, interactive RH used elsewhere. We emphasize that this prescribed RH is only used to compute the radiation and that the model has a full hydrological cycle with an internally determined RH otherwise. As a validation of this approach, the asymmetric climate produced is nearly identical to that of the control run when the prescribed RH is taken to be the climatological RH from that simulation (cf., dashed and solid black lines in Figure 3).

We examine two classes of simulations in which the prescribed RH field is manipulated to investigate how its asymmetry controls the asymmetric climate. In one of these, we maintain the location of the RH maximum produced by the ITCZ but modify the asymmetry in the subtropical RH field. In the other, the latitude of the ITCZ RH maximum is moved north or south holding the subtropical RH values unchanged.

To manipulate the subtropical asymmetry in RH, we first compute the linear slope in RH in the control climatology between the ITCZ and 30° latitude independently for each hemisphere and at each level between 150 and 850 hPa. In the first, "symmetric" simulation, the subtropical RH asymmetry is removed by using multipliers for these trends that equalize the RH minima in the hemispheres, at every level. Figure 3b shows the resulting RH field and Figure 3c its midtropospheric profile (blue line). In a second, "reversed" simulation (red line in Figure 3c), the RH minimum is made deeper in the Northern than in the Southern Hemisphere. At the ITCZ location of the control run, the prescribed RH field is kept unchanged in both simulations.

These changes to the off-ITCZ relative humidity have a large impact on the precipitation field. The ITCZ shift is reduced in the symmetrized simulation and nearly eliminated in the reversed simulation even though the maximum heating is kept unchanged at the location of the control ITCZ by construction. This exercise makes it clear that in our model, the ITCZ latitude is determined by the tropics-wide hemispheric asymmetry in the heating as in the pictures put forward by Lindzen and Hou (1988) and Kang et al. (2008) rather than by the location of maximum heating as in some ITCZ theories (e.g., Waliser & Somerville, 1994). On the other hand, the ITCZ latitude overlies the maximum slab temperature in all these simulations (not shown), consistent with Privé and Plumb (2007) and Singh (2019). In our energetically closed framework, one can think of both the slab temperature and precipitation as ultimately being determined by the TOA heating.

In the second set of simulations, we shift the location of the RH maximum as seen by the radiation but also stretch or compress the meridional coordinate so as to keep RH unchanged at this location and at ±30°. We shift the RH maximum by $\pm\Delta/2$ and $\pm\Delta$, where $\Delta \approx 8°$ is the meridional ITCZ shift in the control climatology, so that with a $-\Delta$ shift the RH maximum moves back to the equator ("unshifted" RH, Figure 4b). The RH profiles for all these cases are shown in Figure 4c and the corresponding results in Figures 4d–4f. In particular, we find that the ITCZ of the unshifted simulation still resides in the Northern Hemisphere even though the net heating peaks at the equator by construction. In addition, these simulations suggest that it is difficult to shift the ITCZ further poleward than simulated in the control. Overall, the implication from these manipulated-RH simulations is that

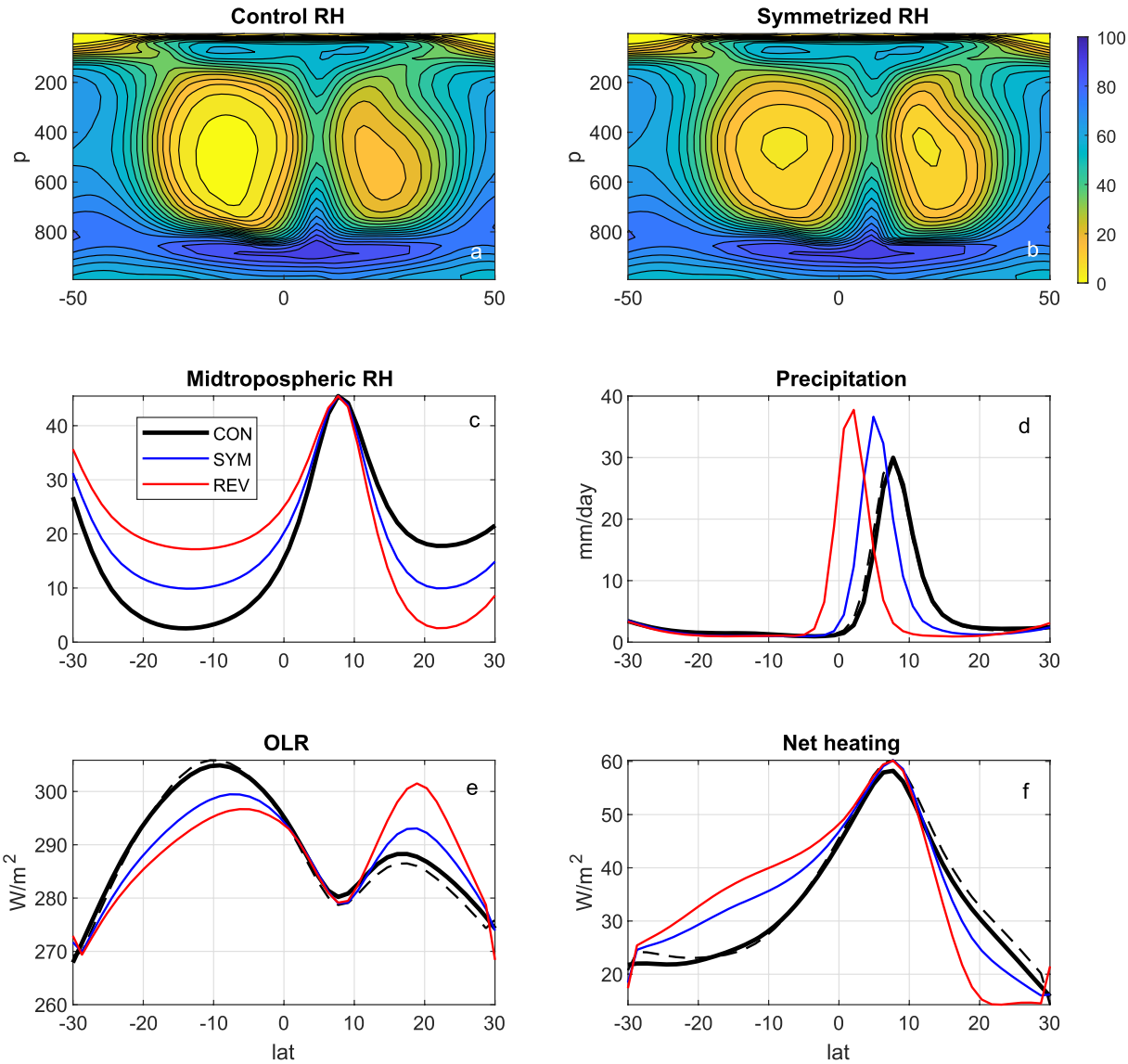

Figure 3. (a) Mean relative humidity profile for the control T85 simulation; (b) Symmetrized RH profile used for the prescribed RH simulations (see text for details); (c) Midtropospheric RH profiles for the control simulation (thick black), a simulation with symmetrized off-ITCZ RH (blue) and a simulation with reversed off-ITCZ RH (red); (d) Same but for the precipitation; (e) Same but for the OLR; (f) Same but for the net column heating. The dashed black line shows the same fields for the control T85 simulation with fully interactive radiation.

the displaced RH maximum and the subtropical RH asymmetry are of comparable importance for the maintenance of the shifted ITCZ.

However, we do not mean to imply that the RH distribution is the only factor controlling the precipitation structure. A comparison of this LSC model with a model using the SBM convective scheme of Frierson (2007b) is illuminating in this regard. We have run the SBM model, using the same setup as in our control except for the convection scheme, prescribing the RH in that model, with the same procedure as described above, to the time-averaged RH produced in our LSC control. The results are described in Figure 5. The heating fields and associated total atmospheric energy transport are nearly identical in the two models (Figure 5a), so the location of the energy flux equator, where the transport changes sign, is identical as well. But the ITCZ displacement is smaller in the SBM model (Figure 5b), and the energy flux equator provides a good approximation to the ITCZ position in the SBM model but not in the LSC model. When the total atmospheric transport is decomposed into mean and transient eddy components, the two models look very different. The LSC model produces a poleward moist static energy (MSE) transport from the energy flux equator to the ITCZ by the mean Hadley cell (blue line

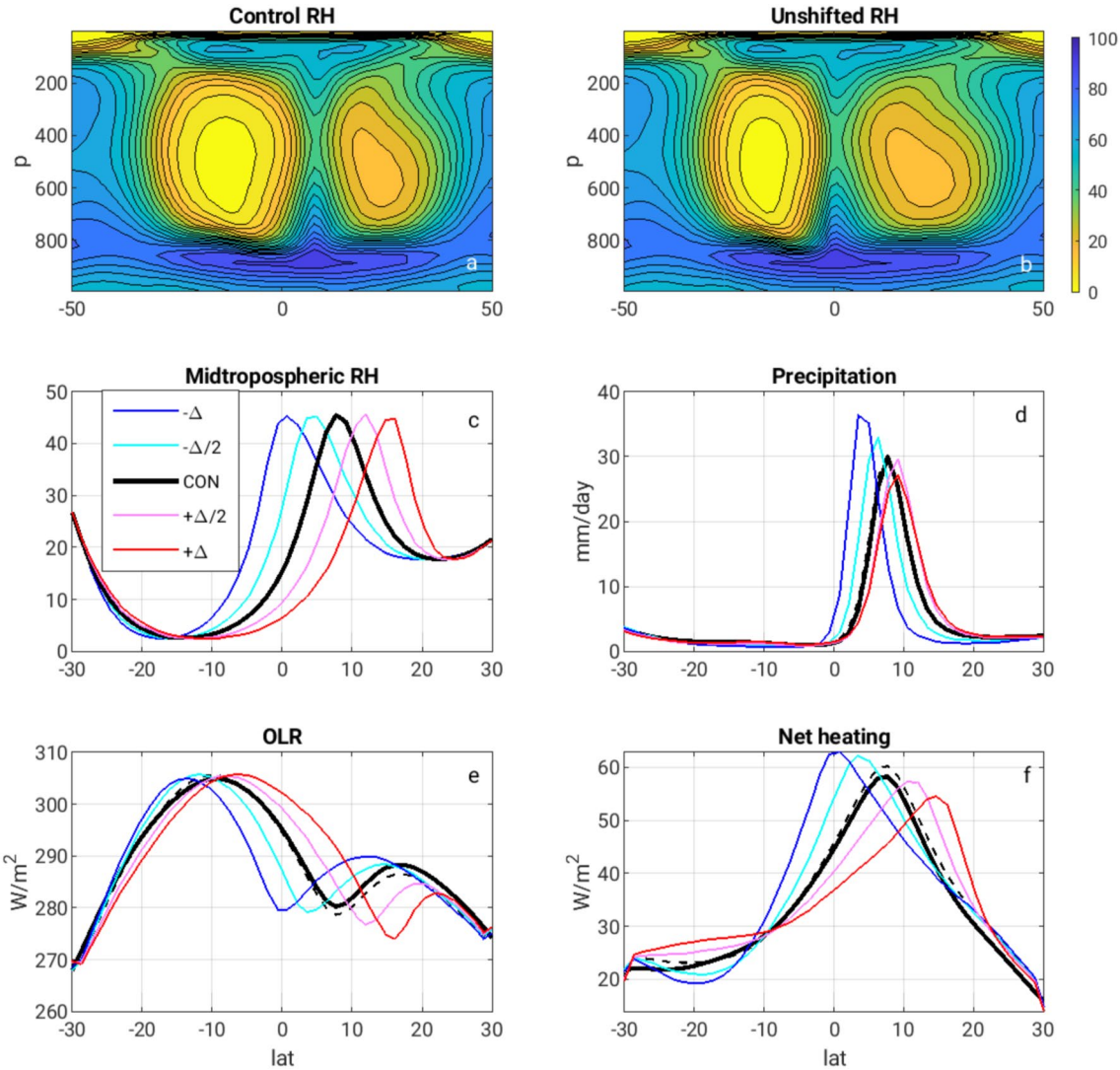

Figure 4. (a) Mean relative humidity profile for the control T85 simulation; (b) Perturbed RH profile obtained shifting the RH maximum back to the equator; (c) Midtropospheric RH profiles for the control simulation (thick black), and simulations shifting the RH maximum distances Δ/2 or Δ equatorward or poleward of its control location, where Δ is the ITCZ shift for the control run; (d) Same but for the precipitation; (e) Same but for the OLR; (f) Same but for the net column heating. The dashed black line shows the same fields for the control T85 simulation with fully interactive radiation.

in Figure 5c). This transport is compensated by transient eddy fluxes (red), which are dominated by moisture fluxes in the deep tropics (not shown). In contrast, the SBM simulation has mean transport away from the ITCZ and much weaker eddy fluxes in the deep tropics (Figure 5d). We can describe the LSC model as having negative Gross Moist Stability (GMS) for the mean flow near the ITCZ, while the convection scheme in the SBM model maintains a positive GMS throughout. We return to the SBM model, with free-running rather than prescribed RH, in Section 5.

4. Sensitivity to Resolution and Other Model Parameters

4.1. Impact of Resolution

We have repeated our control calculation for both lower and higher resolutions: T42, T63, T127, T170, T213, and T255. Clear ITCZ drifts are found for all resolutions up to T170 (fourth panel in Figure 6) but the T213 and T255 simulations do not show a clear shift.

Figure 7a compares the equilibrium precipitation for all runs (simulations with southern ITCZs are shown reflected across the equator to facilitate comparison). The changes with increasing resolution are modest for

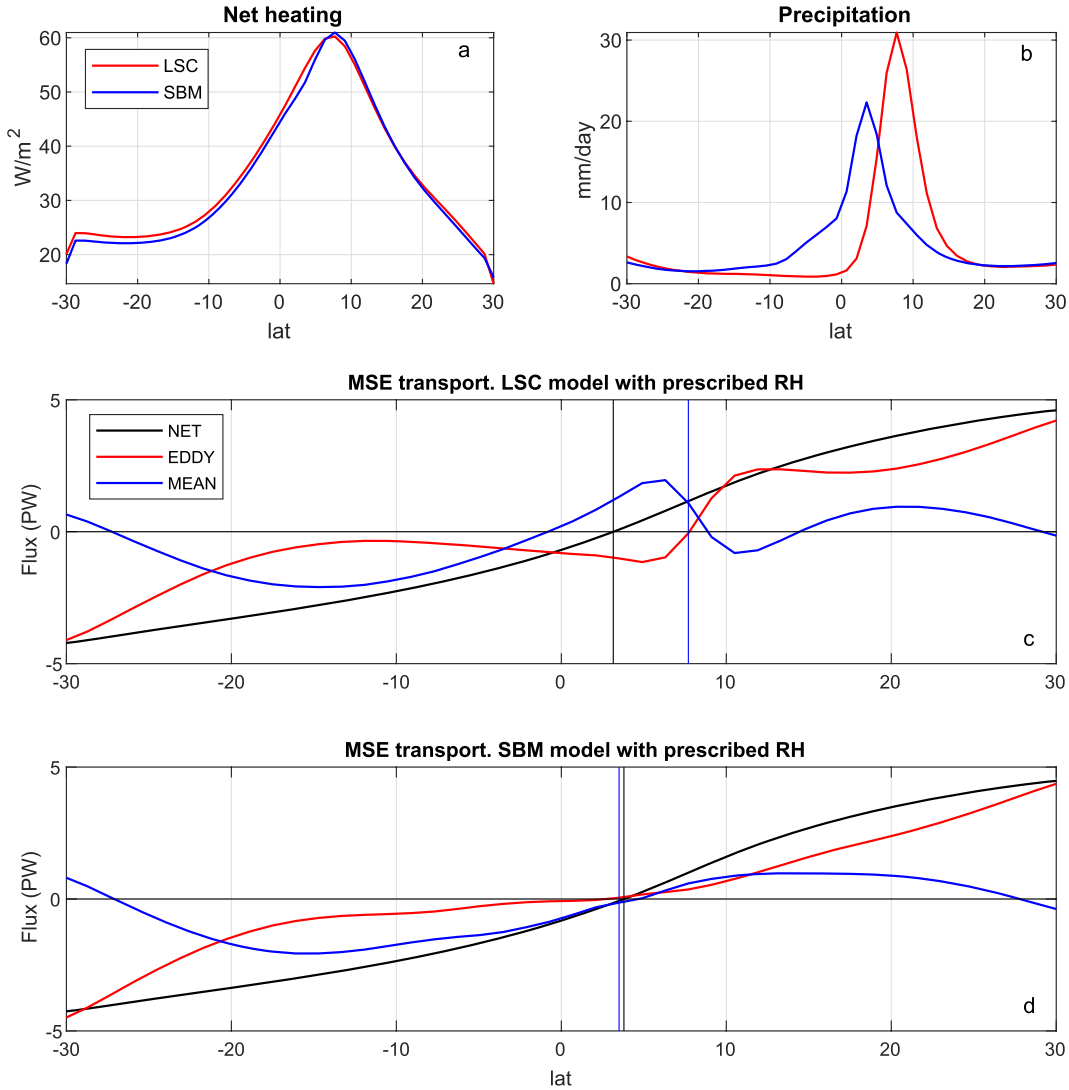

Figure 5. (a) Net column heating and (b) precipitation for LSC (red) and SBM simulations (blue) with prescribed RH taken from the control run. (c) Net moist static energy flux (black) and contributions by the mean circulation (blue) and transients (red) for the LSC simulation with prescribed RH. The black and blue vertical lines show the energy flux equator (latitude of zero MSE flux) and ITCZ (latitude of maximum precipitation), respectively. (d) Same but for the SBM simulation with prescribed RH.

all shifting runs, with small reduction in the ITCZ displacement and with some narrowing of the ITCZ. These changes provide little forewarning of the disappearance of the cross-equatorial asymmetry at T213.

A possible explanation for these results is that asymmetric equilibria still exist at high resolution but cannot be reached easily due to the reduced meridional ITCZ excursions at these resolutions. To test this hypothesis, the bottom panel of Figure 6 shows the precipitation time series for a T213 simulation initialized using the asymmetric SST from the equilibrated T85 run. There is some hint that a shifted equilibrium might also exist at this resolution, with the ITCZ displaced from the equator by an amount comparable to the ITCZ width, but this conclusion should be regarded with caution given the slow evolution.

Following the ITCZ changes, the RH maximum, OLR minimum and heating maximum also shift with resolution. Shifting the curves so that they all peak at the same latitude for ease of comparison, Figure 7b shows that the heating contracts with enhanced resolution, with small increases in its peak value. We can describe this sensitivity more quantitatively by fitting the curves to a Lorentzian profile of the form:

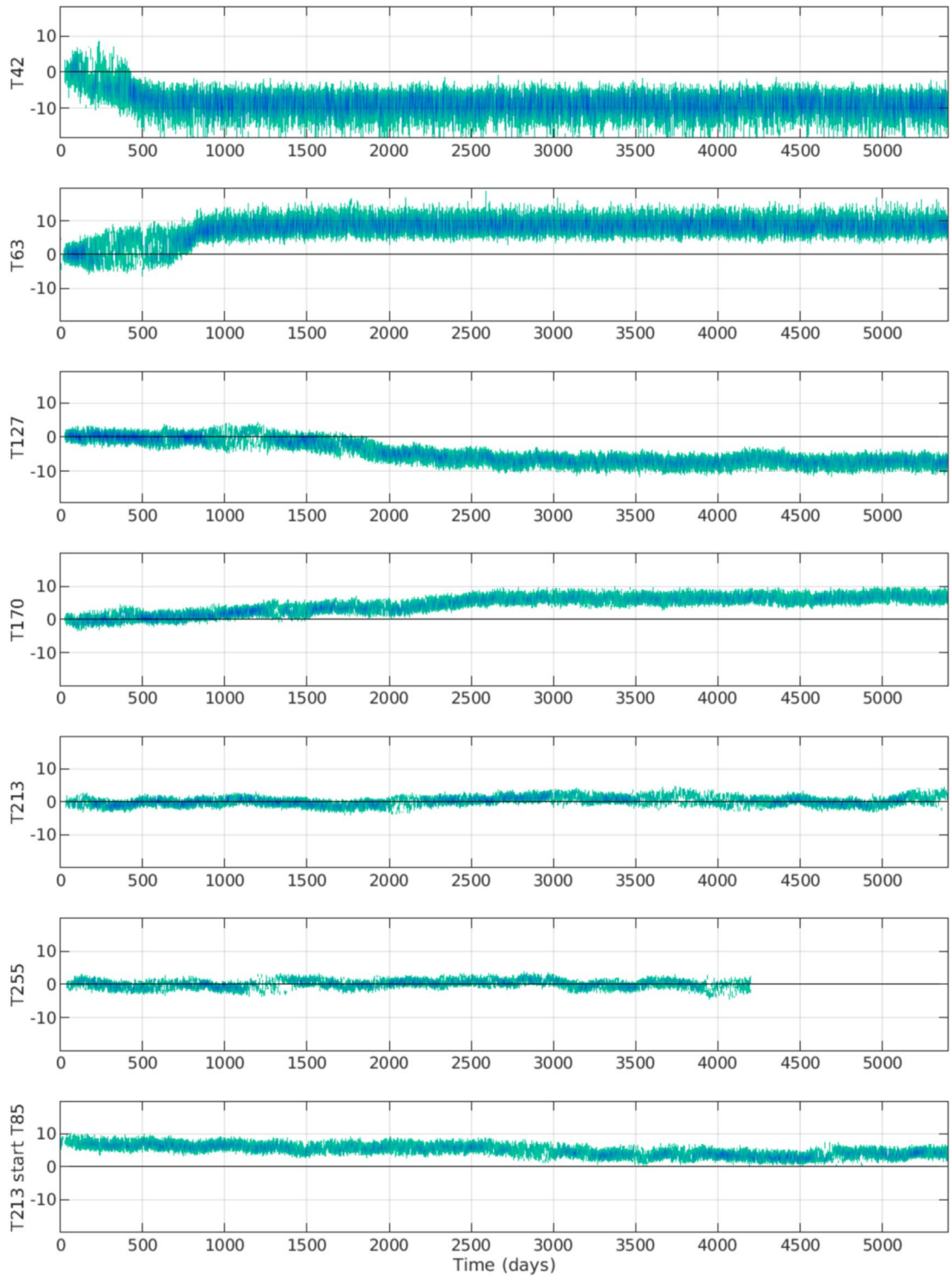

Figure 6. Time series of zonal-mean precipitation at resolutions ranging from T42 to T255. The bottom panel shows the same for a T213 simulation initialized using the equilibrated SST of the control T85 simulation.

$$Q_I = s_I \left[1 + \left(\frac{y - y_I}{w}\right)^2\right]^{-1}, \quad (1)$$

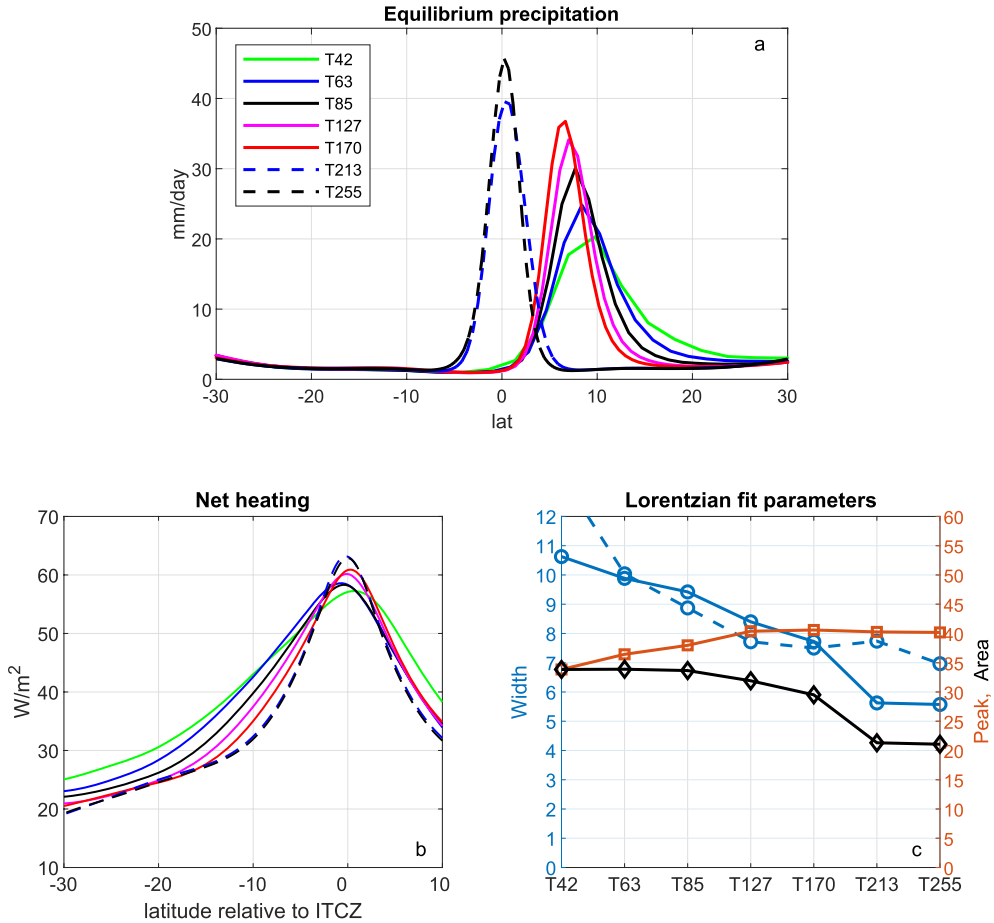

Figure 7. (a) Equilibrium zonal-mean precipitation for simulations with no convective parameterization at various resolutions (see legend). Solid/dashed lines are used to differentiate shifted/symmetric ITCZs. (b) Net heating for the same simulations as a function of distance to the ITCZ. (c) Resolution sensitivity of the Lorentzian best fits to the heating width w (blue) and amplitude s_I (orange) in Equation 1, together with the normalized area (s_I*w/w_{T42}, black). We also show with dashed line the width of the heating in the swamp setting.

Table 1
Summary of Lorentzian Fits to the Heating Width and Net ITCZ Heating[a]

Run	Heating width	ITCZ heating
T42	10.6°	1.00
T63	9.9°	1.00
T85	9.4°	0.99
T127	8.4°	0.94
T170	7.7°	0.87
T213	5.6°	**0.63**
T255	5.6°	**0.62**
$Ri_c = 0.25$	7.3°	**0.74**
REEVAP	7.2°	**0.80**
SBM	12.3°	**2.78**

Note. Stable simulations in bold.
[a]Estimated as the product $s_I w$ in Equation 1 and normalized with the T42 results.

where $y - y_I$ is an ITCZ-relative latitude while s_I and w are fitting parameters. (We also included in our fit a constant term associated with the subtropical heating that was found to change weakly with resolution). An example of this fit is shown with dashed line in Figure 2d for the T85 simulation.

Comparing these parameters for all runs (Figure 7c), we can see that w is reduced by nearly 50% going from T42 to T255, while s_I increases by less than 10%, implying a reduction in the integrated ITCZ heating (black line, see also Table 1). The suggestion from these results is that increased width of the ITCZ-related radiative heating favors the existence of an asymmetric solution. This result can also be described in terms of the latitudinal integral of the heating, larger values of which favor the existence of an asymmetric state. We return to these suggestions in Section 6.

Given the work of Williamson and Olson (2003) on the sensitivity of double-ITCZ solutions in aquaplanets to the physics time step, we have conducted a limited investigation of the timestep dependence in our T85 model. We do not use a split time step in these simulations, with both dynamic and moist physics tendencies computed every 5 min, the maximum value that insures numerical stability as determined by trial and error. (The radiation time step

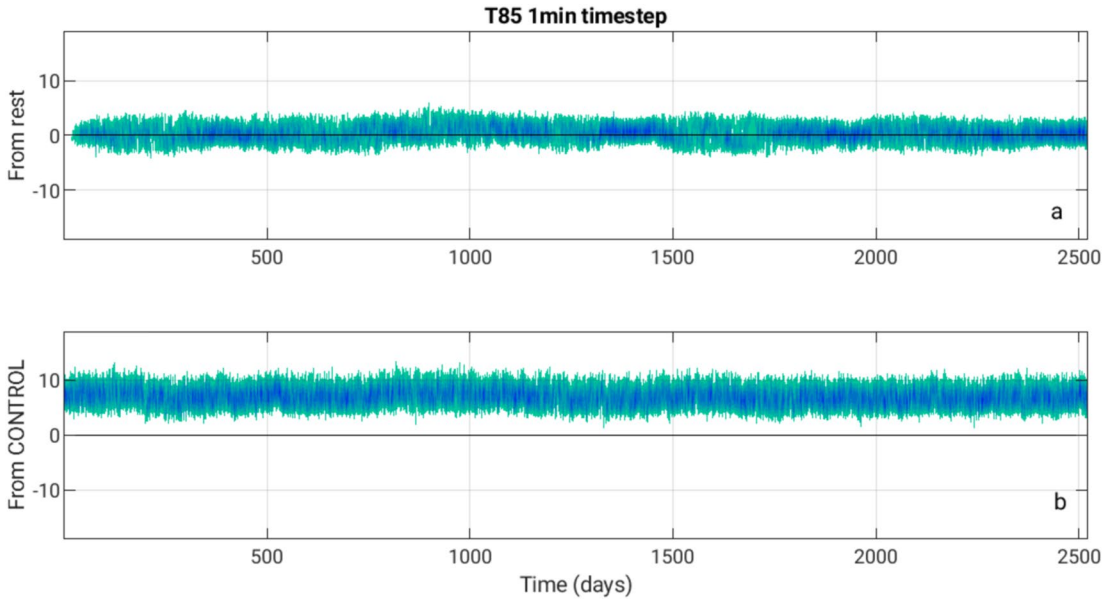

Figure 8. Time series of zonal-mean precipitation for T85 simulations run with 1-min timestep and started from (a) rest or (b) the converged control simulation.

is fixed at 2 hr in all runs.) Reducing the timestep to 1 min, we find the surprising behavior depicted in Figure 8. While the 5-min step results in an asymmetric climate only, the 1-min step model exhibits hysteresis, producing either an equatorial ITCZ or a single off-equatorial ITCZ depending on initial conditions. (We have produced the asymmetric climate in the figure by initializing with the SSTs from the final equilibrated state in the control run.) A third equilibrium with a single southern hemisphere ITCZ can also be obtained by reversing the initial conditions (not shown).

Simulations with time steps intermediate between 1 and 5 min suggest that a smaller time step tends to stabilize the symmetric climate, increasing the time required to transition to the asymmetric state. Preliminary tests at other resolutions provide a consistent picture of the delicacy of the stability/metastability/instability of the symmetric state to time step but with relatively little sensitivity of the structure of the asymmetric states. In the T42 model, we find only asymmetric states for all timesteps down to a few seconds.

We have found only very weak sensitivity to the strength of the scale-dependent damping of small scales in this spectral model. But there may be sensitivity to other numerical aspects of the model, such as vertical resolution (Retsch et al., 2017) or the dynamical core formulation, that we have not examined.

4.2. Surface Heat Capacity

We have found that the instability of the equatorial ITCZ requires that the slab ocean have a critical amount of thermal inertia. Our control simulations use a heat capacity corresponding to 20 m of water, relatively large compared to what is commonly used in this class of idealized models, in which shallower slabs are usually motivated by the desire of minimizing the time required to equilibrate. When this heat capacity is reduced substantially in our model, the instability is inhibited. This is illustrated by Figure 9, which shows time series of zonal-mean precipitation at T85 resolution for select slab depths. In the limit $H = 0$, which we refer to as a "swamp" following Manabe (1997), the peak in zonal-mean precipitation varies only modestly around the equator on fast time scales. As H increases, the ITCZ starts drifting off the equator, initially in sporadic short-lived episodes (0.5 m) and then quasi-periodically (1 m). For larger values of H, the ITCZ shifts to an off-equatorial position, where it persists for a prolonged time, but it sporadically returns to the equator to subsequently undergo a new transition (see 1.5 m). For $H \geq 2$ m, the ITCZ shift appears to be irreversible. These simulations have been extended longer than shown in the figure, up to as long as 10,800 days, with no changes in this qualitative behavior.

The 2 m threshold implies that the ITCZ shift requires a slab heat capacity comparable to or larger than the atmospheric heat capacity, $O(10^7\ \mathrm{J\ K^{-1}\ m^{-2}})$. Interestingly, a transition from non-aggregating to aggregating convection

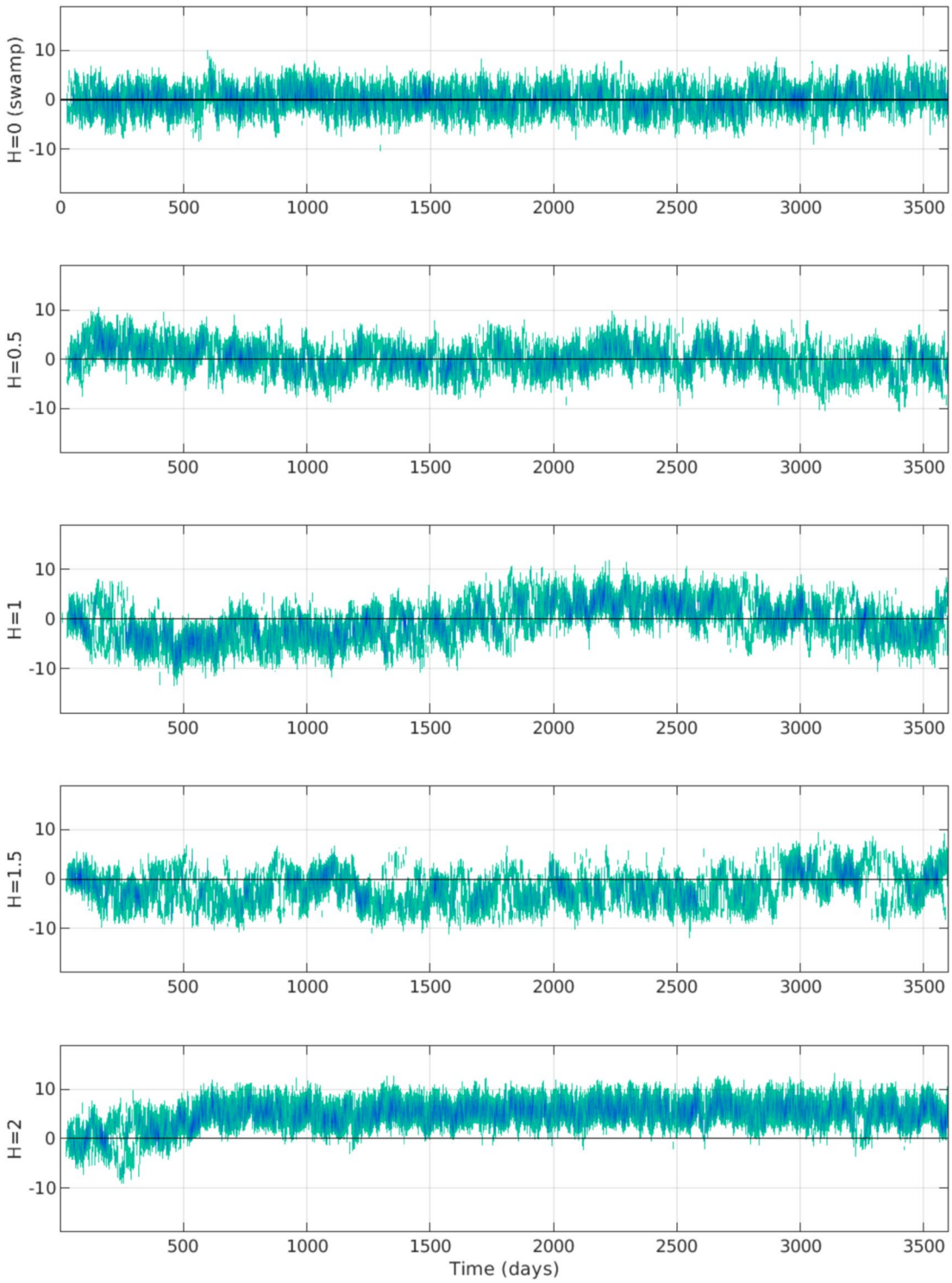

Figure 9. Time series of zonal-mean precipitation for T85 simulations with no convective parameterization and varying slab depth.

as the slab depth is increased has been found in simulations of radiative-convective equilibrium (with the transition at similar depth as here: between 1 and 5 m in Hohenegger and Stevens (2016) for example). Hohenegger and Stevens (2016) attribute this transition to an increase in spatial SST variability that alters the competition between evaporation and the export of moisture by shallow low-level circulations in the non-convective regions. But we have no evidence that this mechanism is relevant in our inhomogeneous setup.

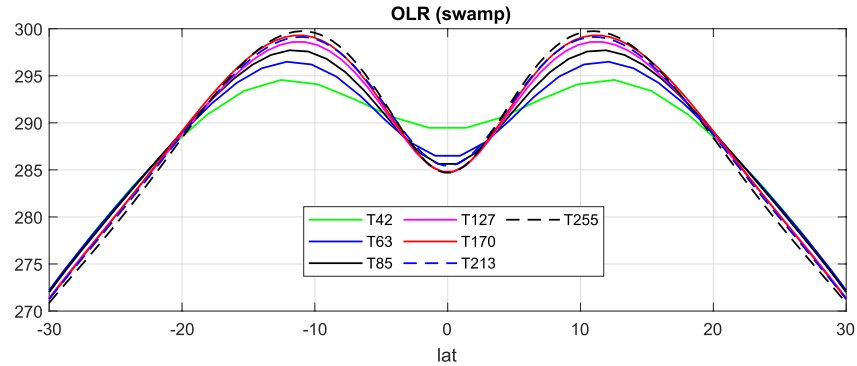

Figure 10. Equilibrium OLR (W m^{-2}) for swamp simulations with no convective parameterization at various resolutions. Dashed/solid lines indicate resolutions with stable/unstable ITCZ with the control slab depth.

We have repeated this H variation at different horizontal resolutions, holding other parameters in the control model fixed. The results are qualitatively similar in that simulations with $H < 2$ m have a stable symmetric climate. But the transition to instability seems to occur at larger depths at higher resolution. We have not attempted to identify the transition depth in these cases more precisely due to the large cost at high resolution of the long integrations needed to distinguish the different types of behavior seen in Figure 9.

The $H = 0$ swamp limit provides a clean hemispherically symmetric climate with little low-frequency variability to compare the impact of different modeling choices on the tropical humidity distribution and closely related OLR fluxes. Potentially, one could look for signatures in these swamp simulations that predict whether models with deep slabs produce asymmetric climates. Figure 10 shows the OLR in the swamp limit for all resolutions from T42 to T255. All of these simulations produce an equatorial ITCZ.

We noted above that the heating narrows with increasing resolution (blue line in Figure 7c). However, this may be partly due to the increased generation of waves and vortices when the ITCZ drifts off the equator. To investigate this possibility, we also include with dashed line in Figure 7c the Lorentzian fits to the heating width for the swamp simulations, all which have an equatorially centered ITCZ. For resolutions T127 and lower the sensitivity is comparable to that in the control $H = 20$ m setting, suggesting that the width sensitivity in that setting is not caused by differences in the ITCZ latitude.

4.3. Prescribed Poleward Heat Transport in the Slab Ocean

To the extent that the existence and structure of asymmetric climates in this model are controlled by the energy balance, as indicated by the relative humidity manipulations described in Section 3, we expect sensitivity to the addition of a prescribed Q-flux to the slab. We consider only symmetric redistributions of heat confined to the tropics. Following Merlis et al. (2013b), we model the convergence of the ocean heat flux as:

$$-\nabla \cdot F_{OCEAN} = \frac{Q_0}{\cos\phi}\left(1 - \frac{2\phi^2}{\phi_0^2}\right)\exp\left(-\frac{\phi^2}{\phi_0^2}\right) \tag{2}$$

with $\phi_0 = 16°$. We consider both positive and negative values for Q_0 (warming the equator and cooling the subtropics or the reverse).

The instability is favored by poleward Q fluxes that cool the equator (as happens in nature). With $Q_0 = -20$ W m^{-2}, the ITCZ transition occurs earlier for the control T85 simulation (Figure 11a, note the different time range from Figure 1) and the instability persists at higher resolution than for the control setting (the T213 simulation is now unstable, see Figure 11b).

Consistently, an equatorward Q-flux can stabilize an equatorial ITCZ. For the control T85 resolution, this requires a minimum $Q_0 = 8$ W m^{-2} (Figure 11c). But we have found some hysteresis as well. Initializing the $Q_0 = 8$ W m^{-2} simulation with the asymmetric climate obtained with $Q_0 = 6$ W m^{-2} instead, the shifted ITCZ can be maintained (Figure 11d). Just as for the timestep dependence, the effect may be better described as affecting the stability or metastability of the symmetric state more significantly than the asymmetric equilibria.

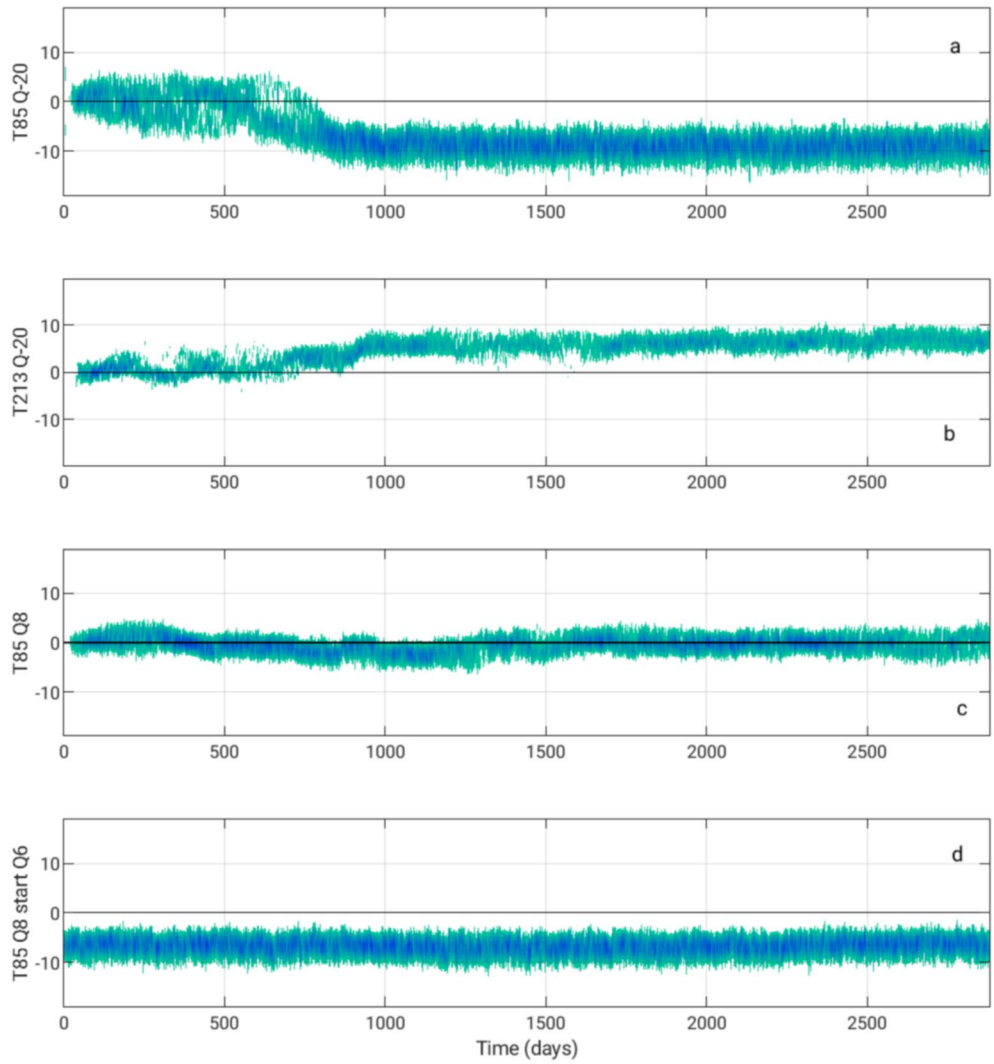

Figure 11. Timeseries of zonal-mean precipitation for: (a) A T85 simulation with poleward Qflux 20 W m^{-2}; (b) A T213 simulation with poleward Qflux 20 W m^{-2}; (c) A T85 simulation with equatorward Qflux 8 W m^{-2}; (d) Same as (c) but starting from the equilibrated climate obtained with an equatorward Qflux 6 W m^{-2}.

4.4. PBL Depth

The instability of the equatorial ITCZ state also has some sensitivity to the configuration of the model's planetary boundary layer (PBL). In particular, a shallower PBL than generated in the control can inhibit the ITCZ instability from appearing. To probe this sensitivity, we run further simulations in which we perturb the critical Richardson number Ri_c of the PBL scheme from its control value of $Ri_c = 1$. The point at which the Richardson number of the flow exceeds Ri_c marks the top of the PBL (the height where the turbulent diffusivities go to zero). Changing the value of Ri_c represents the primary way in which the model's PBL scheme can be smoothly perturbed. Figure 12 shows time series of zonal-mean precipitation for experiments run at T85 resolution with Ri_c set to 1 (its control value) and 0.25. We have performed simulations at other values and resolutions as well, and the ITCZ instability is consistently inhibited for smaller values of Ri_c, corresponding to a thinner boundary layer relative to the control value.

Figure 13a shows how changing Ri_c alters the RH distribution in the swamp setting. Here it can clearly be seen that using a smaller value of Ri_c leads to a shallower PBL, enhancing OLR away from the equator (Figure 13b). The ITCZ, in contrast, is slightly moistened. As a result, the ITCZ stabilization with decreasing Ri_c is accompanied by a sharpening of the OLR as previously found for the resolution sensitivity. Associated with this sharpening, the heating width estimated using Equation 1 reduces by about 20% (from 9.4° to 7.3° at T85) and the net ITCZ heating decreases (Table 1).

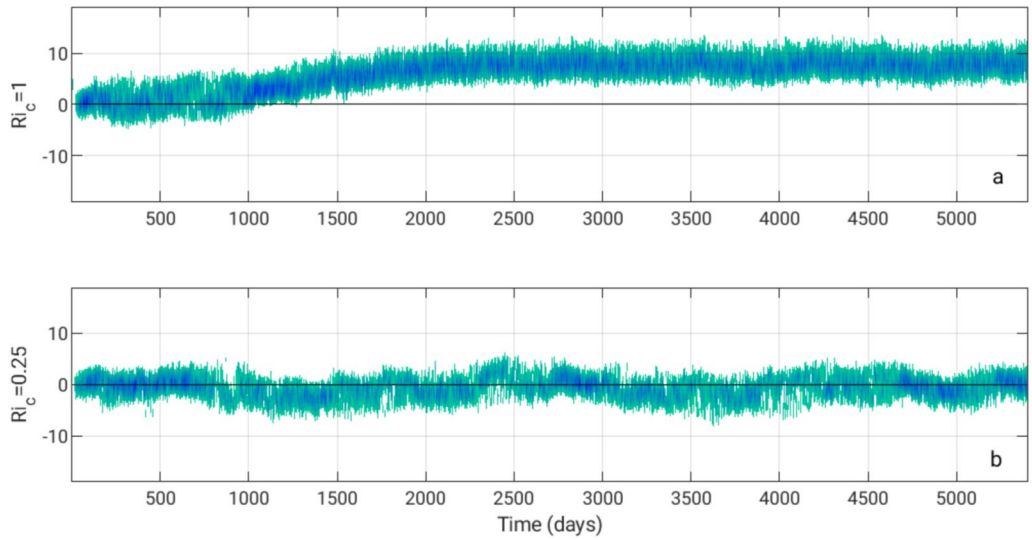

Figure 12. Time series of zonal-mean precipitation at a resolution of T85 for Ri_c values of (a) 1 and (b) 0.25.

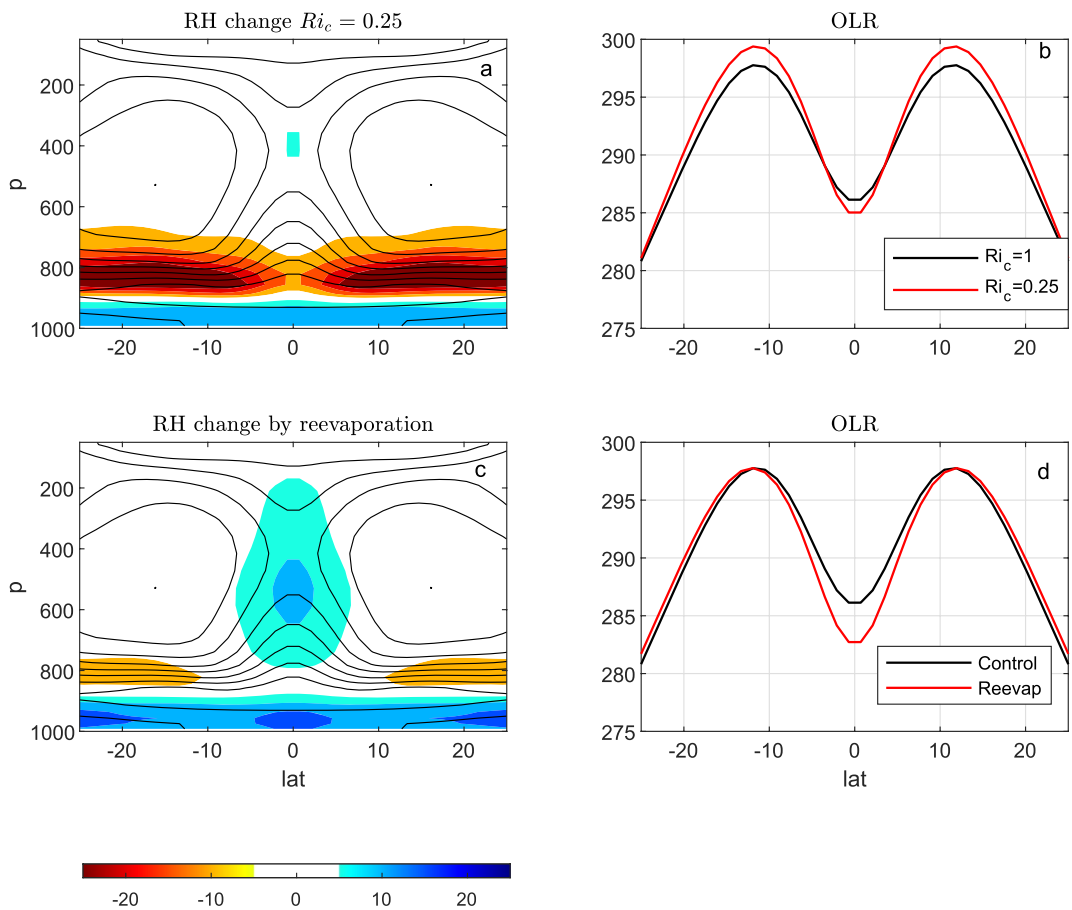

Figure 13. (a) Climatological relative humidity for the control swamp simulation with Ri_c = 1 (black contours every 10%) and RH changes when Ri_c is reduced to 0.25 for T85 resolution simulations; (b) OLR for the control swamp simulation (black) and for the simulation with Ri_c = 0.25 (red); (c, d) as above but when enabling rain reevaporation.

4.5. Evaporation of Condensate

Another factor impacting the RH distribution in the model is the treatment of condensate. In the control configuration used above, the liquid water is immediately rained out upon condensation. But the model also allows an alternative configuration in which the falling rain is reevaporated. In this opposite extreme limit, the precipitation only reaches the surface when the column is fully saturated below the level of condensation.

This has the expected impact on the model's RH and has also been found to affect the ITCZ instability, which only survives for the lowest resolutions (up to but not including T85) with rain reevaporation. Figure 13 shows the impact of this modeling choice on the RH distribution (bottom left) and OLR (bottom right) using the swamp setting. The most obvious RH impacts are a moistening at the ITCZ latitude that deepens the OLR minimum and a slight shallowing of the BL in the subtropics. This increases the ITCZ-to-subtropics OLR gradient, makes the ITCZ heating narrower ($w = 7.24°$) and reduces the net ITCZ heating (cf., Table 1), again consistent with the changes seen in the resolution and Ri_c sensitivity experiments for the stable simulations.

5. ITCZ Instability With the Simplified Betts-Miller Scheme

As discussed in the introduction, several previous studies have used idealized moist GCMs with realistic radiation similar to our model. However, the majority of these studies parameterize the convection using the simplified Betts-Miller (SBM) scheme of Frierson (2007b). The ITCZ instability described in this paper has not been reported using that configuration to our knowledge. We have confirmed that the ITCZ instability does not occur with the standard configuration of the SBM scheme at any resolution in the range that we have analyzed in the LSC model. Figure 14 shows results for the SBM analog of the T85 control run. The ITCZ is very stable: it weakens sporadically but rarely moves from the equator. Even with strong poleward Q fluxes $Q_0 = 40$ W m^{-2}, the ITCZ wobbles between the two sides of the equator but never sets into an asymmetric equilibrium (not shown).

As shown in Figure 14, the SBM model produces much larger RH in its ITCZ than the LSC model (shown dashed for comparison) and hence a much deeper OLR minimum (35 W m^{-2} compared to 10–25 W m^{-2} in the LSC model). As the SBM model also has wider heating than its LSC counterpart, this model produces substantially stronger ITCZ heating (Table 1).

This is at odds with the stabilization found in other parameters settings, which is always accompanied of a reduction in the net ITCZ heating. This suggests that other factors, like the different sign of GMS with the SBM scheme and with LSC only (cf., Section 3 and Figure 5), may also play a role for the different ITCZ stabilities of the two models. It is tempting to speculate based on these results that the negative GMS of the LSC setting might be key for the instability more generally, but examination of the GMS in some of the other simulations described above produces mixed results. For instance, the analysis of the sensitivity to the PBL depth shows that a shallower PBL stabilizes the ITCZ despite decreasing (i.e., even more negative) GMS (not shown).

The stability of the symmetric climate with the SBM convective scheme is robust over a wide range of parameters. We could not destabilize the model by disabling shallow convection or by changing the reference relative humidity of the scheme. The model can be destabilized by increasing the relaxation timescale but this requires timescales of several days, much longer than needed to make resolved precipitation dominate over convective precipitation.

Motivated by the conjecture that the ITCZ stability in the SBM model might be partly due to its large GMS, we tried a modification of the SBM scheme relaxing to a profile less stable than the moist adiabat. Specifically, we tried relaxation to a profile defined by the following lapse rate:

$$-\frac{dT}{dz} = \mu\Gamma_m + (1-\mu)\Gamma_d \tag{3}$$

where Γ_d (Γ_m) is the dry (moist) adiabatic lapse rate and the standard SBM scheme is recovered with $\mu = 1$. Using this modification, it is possible to destabilize the scheme with modest reductions in μ. The critical μ depends on resolution: $\mu = 0.8$ at T42 and $\mu = 0.6$ at T85. We have verified that for these values of μ the convective scheme still provides significant vertical MSE transport, so that the destabilization of the ITCZ in this limit is not simply due to the scheme becoming inoperative and the model reverting back to LSC.

An alternative, more physical way to destabilize the SBM scheme is by relaxing to the entraining plume profile of Duffy and O'Gorman (2022), calculated assuming that the convective plume is mixed with the environment with

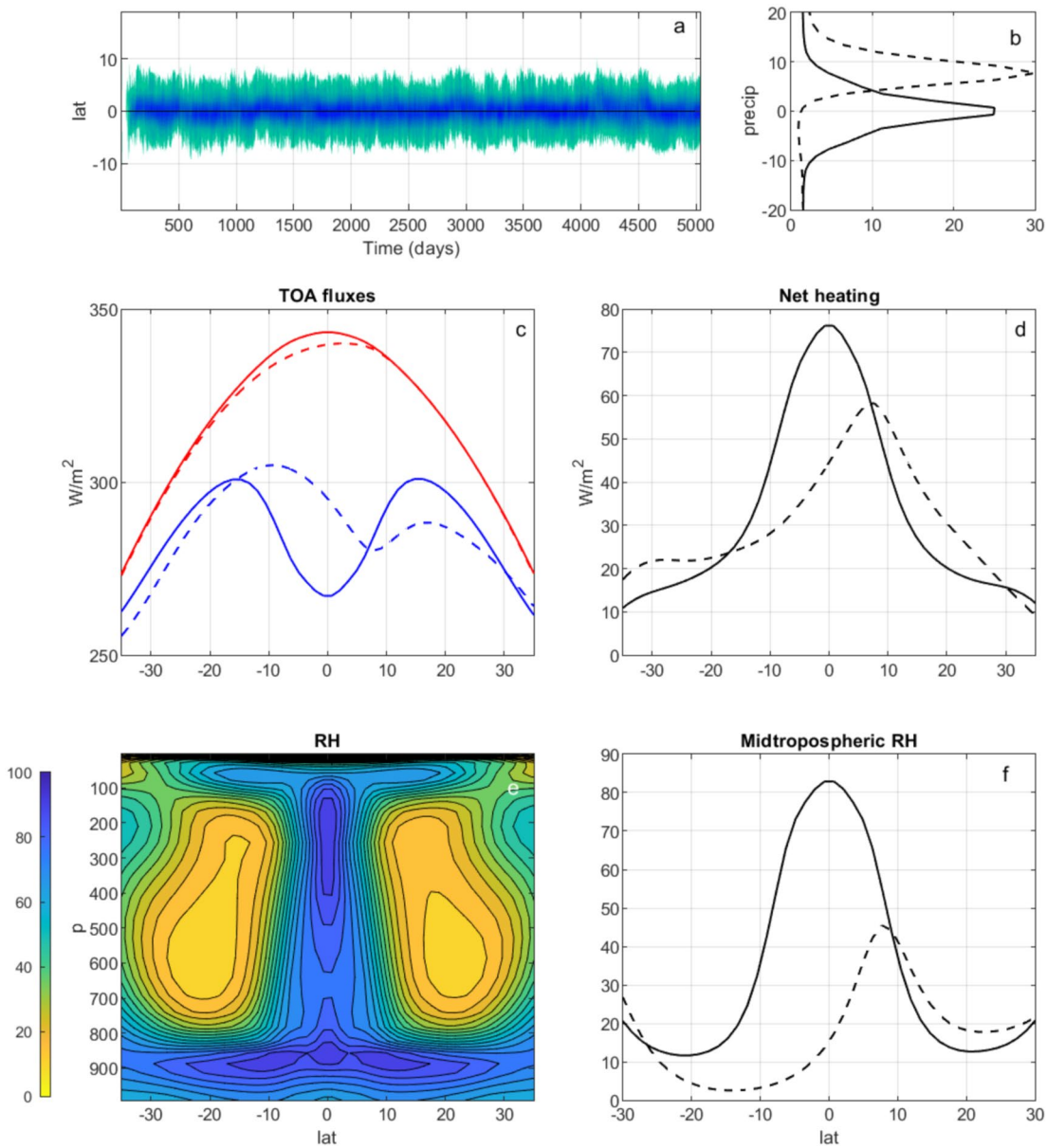

Figure 14. For the T85 simulation using the simple Betts-Miller convective scheme: (a) Time series of zonal-mean precipitation and (b) climatological precipitation; (c) Top of the atmosphere radiative fluxes (red: shortwave, blue: OLR) and (d) net column heating; (e) Climatological relative humidity and (f) its midtropospheric (530 hPa) profile. The dashed lines in all panels show the corresponding LSC results for comparison.

an entraining rate inversely proportional to height. We were also able to destabilize the model using this scheme, though at T85 this required an entrainment parameter an order of magnitude larger than considered by Duffy and O'Gorman (2022) (not shown).

These results suggest that the ITCZ instability may not be unique to the LSC setting and could plausibly also occur under convective parameterizations that do not stabilize the tropics as strongly as the SBM scheme. Zhihong Tang (personal communication) reports encountering this instability when using an eddy-diffusivity/mass-flux parameterization for the convective closure.

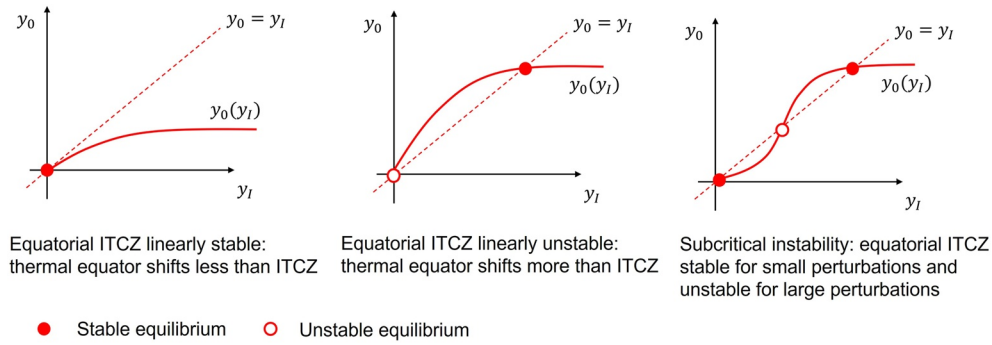

Figure 15. Schematic depicting the sensitivity of the energy flux equator y_0 to the latitude y_I of ITCZ heating under idealized scenarios supporting linear stability (left), linear instability (middle) and subcritical instability (right). The filled (empty) red circles represent stable (unstable) equilibria.

6. Discussion

6.1. The Basic Physical Picture

As the prescribed RH simulations demonstrate, the asymmetric GCM equilibrium is maintained by the asymmetric tropical and subtropical radiative heating associated with an off-equatorial ITCZ. Kang et al. (2008) have shown that with asymmetric heating, the ITCZ must move into the more strongly heated hemisphere to maintain flat deep-tropics temperatures. When the heating is tied to the circulation and not prescribed, we may expect instability if the anomalous circulation driven by the RH-controlled heating asymmetry produced by an ITCZ shift tends to amplify that shift.

Consider for instance a situation in which the ITCZ is displaced to a latitude $y_I > 0$ north of the equator as part of the model's internal variability. The perturbed RH will then make radiative heating asymmetric about the equator and, if this asymmetric heating is maintained long enough for the atmospheric circulation to adjust (which requires sufficient thermal inertia in the slab), this will move the energy flux equator to some latitude y_0 in the Northern Hemisphere. Neglecting eddy fluxes for simplicity (this assumption is relaxed below) the maximum Hadley cell updraft and the ITCZ will drift toward this new latitude.

We can then envision two different scenarios. If $y_0 < y_I$ (Figure 15, this figure and the accompanying discussion were inspired by the comments of Ori Adam), the heating asymmetry is reduced by the circulation and the ITCZ returns toward the equator. On the contrary, when $y_0 > y_I$ the ITCZ is unstable because the induced circulation will make the heating more asymmetric and amplify the initial ITCZ drift (Figure 15, middle). For small perturbations, the ITCZ instability depends on the slope of the $y_0(y_I)$ curve (red solid line) at $y_I = 0$ and can be determined using the asymptotic expansion of Bischoff and Schneider (2014). More generally, one may also envision situations in which the ITCZ is stable for small perturbations and unstable for large perturbations (Figure 15, right), so that more than one stable equilibrium may exist.

6.2. Sensitivity of the Energy Flux Equator to the ITCZ Heating

Based on the above discussion, we expect the instability to be determined by the $y_0(y_I)$ curve (red solid lines in Figure 15). In principle, one could use the prescribed-RH model to map how the energy flux equator changes when the ITCZ RH is shifted. Due to the different RH structure about the ITCZ when the resolution and model parameters are varied, we expect the $y_0(y_I)$ relation to differ across the various settings, affecting the instability of the respective models. Rather than performing this exercise explicitly, we use the tropical energy balance to analyze what determines the sign of $y_0 - y_I$.

Consider first a situation in which the ITCZ RH has no radiative impact, for instance when RH is constant or when using gray radiation. The energy balance in this situation is given by:

$$S(y) - OLR_0(y) = \nabla \cdot F \tag{4}$$

where $S(y)$ is the solar heating, F is the vertically integrated meridional moist static energy flux and $OLR_0(y)$ the outgoing longwave radiation. We use the 0 subscript to emphasize that this OLR depends only on temperature.

Due to the weak rotation, we expect the meridional structure of temperature and OLR_0 to be strongly constrained by angular momentum conservation and very flat in the deep tropics. If we were given the value of F at the Hadley cell edge, F_H, we could determine OLR_0 by simply shifting this curve as in the classical Held and Hou (1980) solution, equivalent to solving:

$$\langle S \rangle - \langle OLR_0 \rangle = 2F_H, \tag{5}$$

where $\langle \cdot \rangle$ denotes a tropics-wide integral.

In the presence of ITCZ-induced RH structure temperatures are still flat, but OLR no longer is. We take into account the OLR structure due to the water vapor longwave heating by introducing an additional heating term Q_I:

$$S(y) - OLR_0(y) + s_I Q_I(y - y_I) = \nabla \cdot F, \tag{6}$$

where the heating is a function of distance to the ITCZ latitude y_I, and s_I is a measure of the strength of the RH-driven OLR correction. For the sake of concreteness, we make use of the empirical result that Q_I is well approximated by a Lorentzian:

$$Q_I(y) = \frac{1}{1 + \frac{y^2}{w^2}} - 2w \arctan\left(\frac{L_H}{w}\right). \tag{7}$$

This expression differs from Equation 1 by a constant (last term on the RHS), introduced to make $Q_I(y)$ integrate to zero over the tropics (L_H is the Hadley cell width). This allows determining the reference OLR_0 by tropics-wide energy conservation as in Equation 5, assuming that the energy flux at the Hadley cell edge F_H does not change. More generally, we assume that OLR_0 is not affected by changes in the ITCZ latitude y_I. We also assume that the parameters defining the ITCZ radiative heating, s_I and w, are not a function of y_I.

Putting everything together:

$$Q_B(y) + \frac{s_I}{1 + \frac{(y - y_I)^2}{w^2}} = \nabla \cdot F, \tag{8}$$

where $Q_B(y) = S - OLR_0 - 2s_I w \arctan\left(\frac{L_H}{w}\right)$ is a background heating, independent of the ITCZ position under our assumptions.

To understand how the energy flux equator varies when the ITCZ moves, it is useful to consider the integrated energy balance over each of the two Hadley cells. In the unperturbed symmetric climate with $y_I = 0$, the ITCZ heating is equally redistributed between the two cells. The net integrated heating (including this ITCZ term) over either one of the two symmetric cells equals the MSE export F_H across their poleward edge:

$$\int_{-L_H}^{0} Q_B dy + s_I w \arctan\left(\frac{L_H}{w}\right) = \int_{0}^{L_H} Q_B dy + s_I w \arctan\left(\frac{L_H}{w}\right) = F_H \tag{9}$$

Assuming that F_H does not change, the integrated energy balance over each of the two cells is also unchanged when the ITCZ heating moves to the latitude $y_I > 0$ and the Hadley cell boundary moves to the latitude y_0, satisfying

$$\int_{-L_H}^{y_0} Q_B dy + \int_{-L_H}^{y_0} \frac{s_I dy}{1 + \frac{(y - y_I)^2}{w^2}} = \int_{y_0}^{L_H} Q_B dy + \int_{y_0}^{L_H} \frac{s_I dy}{1 + \frac{(y - y_I)^2}{w^2}} = F_H \tag{10}$$

Focusing on the southern Hadley cell, for $y_0 > 0$ the first integral on the LHS decreases when Q_B is negative and increases when it is positive relative to the symmetric case. To keep the cell-wide integrated heating unchanged, these changes must be compensated by the second integral on the LHS. Thus, y_0 must be larger (smaller) than y_I when Q_B is negative (positive), so that more (less) of the ITCZ heating goes into the southern cell. We conclude that the instability is determined by the sign of the background heating $Q_B(y)$. The same conclusions are reached if we focus on the northern Hadley cell instead.

This result is qualitatively consistent with the GCM simulations. A negative Q_B at the equator requires:

$$S(0) - OLR_0(0) \leq 2s_I w \arctan\left(\frac{L_H}{w}\right), \tag{11}$$

so that the instability is favored when the background equatorial heating $S - OLR_0$ decreases (as in the presence of a poleward Q-flux) and with large integrated ITCZ heating $s_I w$. Neglecting the meridional structure of $S - OLR_0$ compared to that of Q_I, we can estimate this heating using the Lorentzian fit in Equation 1. As discussed in Section 4 and summarized in Table 1, the integrated ITCZ heating decreases when resolution is enhanced, when the critical Richardson number is decreased and when rain reevaporation is enabled. All these changes were found to stabilize the ITCZ in the GCM simulations.

6.3. Stabilizing and Destabilizing Feedbacks

The simulations using the SBM convective scheme seem to contradict the above result. These simulations have a stable ITCZ despite producing the largest ITCZ heating by far across all our runs (Table 1). The very different decomposition of the MSE transport in this setting and with the LSC model (Figure 5) suggests that the role of the eddy moisture fluxes for the latter cannot be ignored.

Because of these eddy fluxes, there is now a MSE transport across the boundary between the two Hadley cells so that they are no longer subject to the same integrated heating. When the ITCZ is located poleward of the energy flux equator as in Figure 5, this eddy MSE transport is directed from the southern to the northern cell (assuming as before a positive y_0). Using similar arguments to those above, it is easy to see that this favors the instability. We can also understand this result in terms of the schematic in Figure 15. When the ITCZ is located poleward of the energy flux equator, that is, $y_I = \alpha y_0$ with $\alpha > 1$, it is only required that $y_0 \geq y_I/\alpha$ for instability, as this will suffice to amplify a spontaneous ITCZ shift. The different stability of the SBM and LSC settings suggests that the large value of $\alpha \approx 2.3$ for the latter is key for its instability. In support of this hypothesis, simulations with prescribed RH similar to those described in Section 3.1 but using the modified SBM scheme described in Section 5 (cf. Equation 3) suggest that the destabilization of this scheme when μ is decreased is associated with a gradual increase in α ($\alpha = 1.3$, 1.9, 2.2, and 2.3 for $\mu = 0.9$, 0.8, 0.7, and 0.6 respectively, at T85).

Circulation-induced changes in the subtropical RH provide another potential destabilizing effect. While our empirical Q_I fit assumes that the ITCZ heating decreases symmetrically on both sides of the ITCZ, the stronger cross-equatorial Hadley cell may reduce RH more strongly in the opposite hemisphere, increasing the cooling in the southern cell relative to the northern one. This again has a destabilizing effect.

In contrast, changes in F_H have a stabilizing effect that may plausibly be important for the equilibration of the instability. The stronger MSE gradients in the northern subtropics is expected to increase F_H in that hemisphere and cool the northern Hadley cell relative to the southern one.

7. Concluding Remarks

We have studied an idealized aquaplanet moist GCM in a hemispherically symmetric configuration with a slab-ocean lower boundary, and have identified an instability that produces an asymmetric climate with the ITCZ localized in one hemisphere. This instability is driven by the coupling between the circulation and radiative heating. Under some circumstances, when the ITCZ moves off the equator as part of the model natural variability, the asymmetric heating produced by the perturbed RH distribution drives an anomalous circulation that amplifies the original ITCZ shift. When this instability is present the climate is non-unique, since the ITCZ can then form on either side of the equator depending on the initial conditions.

The model excludes cloud-radiative interaction, but the interaction between the circulation and the clear-sky radiation controlled by relative humidity (RH) is still sufficient to destabilize the symmetric climate. We have primarily focused on a model with large-scale condensation (LSC) only in this study, in the hope of avoiding the complexity introduced by sensitivity to details of convection parameterizations and of providing a baseline for a study of that sensitivity. However, we have uncovered a variety of sensitivities to parameters in this LSC model.

A T85 spectral model with a slab depth of 20 m serves as our control and provides a clean example of the instability in the LSC model. Replacing the full radiative transfer module with gray radiation stabilizes the symmetric state, showing that it is circulation-radiation feedbacks that generate the instability. Supplementary simulations in which the tropical RH field input into the radiation is manipulated make it clear that the hemispherically asymmetric RH field generated by the asymmetric circulation is essential for the maintenance of the asymmetric states. Specifically, these simulations show that the subtropical as well as ITCZ RH are important for this maintenance,

supporting a picture similar to that described in Lindzen and Hou (1988) and Kang et al. (2008) in which the tropical energy balance as a whole is a controlling factor.

A sensitivity analysis with the GCM uncovers a rich parameter sensitivity. Our main findings are as follows:

- There is sensitivity to the horizontal resolution; the hemispherically symmetric state is stable at T213 resolution and higher, using the control model settings otherwise. However, when initializing the T213 model with the slab temperatures from the T85 final state, the asymmetric state is maintained for as long as we have extended the integration. The implication is that there are three stable climates, one symmetric and two asymmetric at this resolution.
- Decreasing the time step in the T85 control by a factor of 5 also stabilizes the symmetric state but seemingly does not affect the existence of the asymmetric states, resulting in hysteresis and the existence once again of three distinct climates.
- The heat capacity of the slab ocean must be above a critical value to destabilize the symmetric state. This critical value, corresponding to roughly 2 m of water, is comparable to the heat capacity of the atmosphere.
- A shallower boundary layer inhibits the instability, restricting it to lower horizontal resolutions.
- The evaporation of rain is stabilizing. The control model configuration has no rain reevaporation. When it is included, increasing the tropical RH, the instability is once again restricted to lower resolutions.
- The addition of the simple Betts-Miller (SBM) convection scheme inhibits the instability, though it is possible to destabilize the scheme by manipulating its relaxation profile.

It is difficult to study the transition from stability to instability while varying a parameter, since the resulting climate change is invariably of finite amplitude. We have found no cases in which the latitude of the ITCZ position can be placed arbitrary close to the equator by choosing a parameter close to a stability threshold. When one is close to a critical parameter value the ITCZ latitude typically undergoes large fluctuations. An example is provided by the sensitivity to horizontal resolution: although enhanced horizontal resolution reduces the ITCZ shift at resolutions supporting the instability (T170 or less with our control parameters), the transition to an equatorial ITCZ occurs abruptly when resolution increases beyond that point.

It is admittedly disconcerting for numerical aspects of the model to affect the qualitative structure of the model climate. We have studied horizontal resolution and time step, but there may be others. At a minimum, we believe that these results are of importance to those working with similar idealized moist models, since much of the existing literature uses resolutions similar to that of our control simulation. More fundamentally, it remains unclear whether the instability of the hemispherically symmetric climate in the LSC model survives at very fine resolution.

We propose a simple conceptual framework for the instability based on the sensitivity of the energy flux equator to the asymmetric heating perturbations induced by a spontaneous ITCZ shift. Depending on the ITCZ RH structure, the energy flux equator may shift more or less than the ITCZ, amplifying or damping the initial ITCZ drift. As this mechanism requires sufficient thermal inertial in the slab for the circulation to adjust to the asymmetric heating, it may plausibly explain our findings that a minimum depth is required for instability.

Based on these ideas, we use the tropical energy balance to infer that the instability depends on the sign of the background heating, which we may define as the local TOA heating when the ITCZ moves away. Although it is not obvious how to test the theory quantitatively due to the difficulty of defining this background heating, its predictions seem *qualitatively* consistent with the modeled sensitivity. The instability is favored when the background equatorial heating decreases, as in the presence of a poleward slab Q-flux, and when the net ITCZ heating increases, as found with coarse resolution, deep PBL depth and in the absence of rain reevaporation.

There are two important, possibly related, limitations to this theory. First, the theory strictly predicts the sensitivity of the energy flux equator, which only provides a good approximation to the latitude of Hadley cell rising when transient energy fluxes are small in the deep tropics. This is clearly violated in the LSC model (Figure 5). Additionally, the theory is unable to explain why the SBM model is more stable than the LSC model. We can reconcile these results by noting that transients provide a destabilizing feedback when they shift the ITCZ poleward from the energy flux equator. This can be explicitly incorporated in the theory by including an empirical parameter constraining the ratio between the ITCZ latitude and the energy flux equator, although we do not have a clear picture of how this parameter is determined.

Transients are likely also responsible for the resolution sensitivity of the instability, through transient moisture fluxes and through convective organization that modifies the climatological RH values in the ITCZ. In our LSC simulations, the ITCZ width only seems to converge at the highest resolutions examined (T213 and above), in contrast with the convergence at much lower resolution using the SBM scheme (Byrne & Schneider, 2016), and consistent with the relevance of GMS for ITCZ width in the framework proposed by these authors. As the ITCZ GMS is negative in the LSC setting, cooling at that latitude is entirely due to the transients.

Thus, although the essence of the ITCZ instability seems to be sufficiently simple that it can be explained by a simple energy balance model, the underlying interactions between tropospheric relative humidity, the OLR, and the circulation are evidently more complex and likely involve key properties of convection and convective environments like aggregation or gross moist stability. It is possible that other convective schemes are more prone to the instability than the SBM scheme considered here. If so, it will be interesting to study what emergent properties of these schemes control the occurrence of the ITCZ instability.

Data Availability Statement

The GCM simulations described in this work were performed using the Isca model (commit 9560521e1ba5ce27a13786ffdcb16578d0bd00da) maintained by the University of Exeter (Vallis et al., 2018), which is publicly available under a GNU Public License at https://github.com/ExeClim/Isca (Isca development team, 2023). The figures in this manuscript, created using version R2021b of Matlab^R, can be reproduced using the scripts and data stored at the Zenodo repository https://doi.org/10.5281/zenodo.7777604 (Zurita-Gotor, 2023).

Acknowledgments
We thank Zhihong Tan for sharing unpublished results producing the ITCZ instability in a different model, Spencer Clark for useful discussions, and Dargan Frierson, Martin Jucker, and Neil Lewis for their help clarifying the boundary layer treatment in the model formulation. We are also grateful to the editor Tapio Schneider, Ori Adam and two anonymous reviewers for their helpful and constructive comments. Figure 15 and its interpretation were inspired by the comments of Ori Adam in his review of our original submission. P. Zurita-Gotor has been funded by the Spanish Research Agency project DYNWARM (PID2019-109107GB-I00). IMH, TMM, and PZG acknowledge funding support from NSF award AGS 2246700, and SAH acknowledges funding support from NSF award AGS 2123327. The simulations presented in this paper were performed using High Performance Computing resources provided by the Cooperative Institute for Modeling the Earth System, with help from the Princeton Institute for Computational Science and Engineering.

References

Adam, O. (2021). Dynamic and energetic constraints on the modality and position of the intertropical convergence zone in an aquaplanet. *Journal of Climate*, *34*(2), 527–543. https://doi.org/10.1175/jcli-d-20-0128.1

Barsugli, J., Shin, S.-I., & Sardeshmukh, P. D. (2005). Tropical climate regimes and global climate sensitivity in a simple setting. *Journal of the Atmospheric Sciences*, *62*(4), 1226–1240. https://doi.org/10.1175/jas3404.1

Bellon, G., & Sobel, A. H. (2010). Multiple equilibria of the Hadley circulation in an intermediate-complexity axisymmetric model. *Journal of Climate*, *23*(7), 1760–1778. https://doi.org/10.1175/2009jcli3105.1

Bischoff, T., & Schneider, T. (2014). Energetic constraints on the position of the intertropical convergence zone. *Journal of Climate*, *27*(13), 4937–4951. https://doi.org/10.1175/jcli-d-13-00650.1

Bischoff, T., & Schneider, T. (2016). The equatorial energy balance, ITCZ position, and double-ITCZ bifurcations. *Journal of Climate*, *29*(8), 2997–3013. https://doi.org/10.1175/jcli-d-15-0328.1

Byrne, M. P., & Schneider, T. (2016). Energetic constraints on the width of the intertropical convergence zone. *Journal of Climate*, *29*(13), 4709–4721. https://doi.org/10.1175/jcli-d-15-0767.1

Clark, S. K., Ming, Y., Held, I. M., & Phillipps, P. J. (2018). The role of the water vapor feedback in the ITCZ response to hemispherically asymmetric forcings. *Journal of Climate*, *31*(9), 3659–3678. https://doi.org/10.1175/jcli-d-17-0723.1

Duffy, M. L., & O'Gorman, P. A. (2022). Intermodel spread in Walker circulation responses linked to spread in moist stability and radiation responses. *Journal of Geophysical Research: Atmospheres*, e2022JD037382. https://doi.org/10.1029/2022JD037382

Frierson, D. (2007a). Convectively coupled Kelvin waves in an idealized moist general circulation model. *Journal of the Atmospheric Sciences*, *64*(6), 2076–2090. https://doi.org/10.1175/jas3945.1

Frierson, D. (2007b). The dynamics of idealized convection schemes and their effect on the zonally averaged tropical circulation. *Journal of the Atmospheric Sciences*, *64*(6), 1959–1976. https://doi.org/10.1175/jas3935.1

Frierson, D., Held, I. M., & Zurita-Gotor, P. (2006). A gray-radiation aquaplanet moist GCM. Part I: Static stability and eddy scale. *Journal of the Atmospheric Sciences*, *63*(10), 2548–2566. https://doi.org/10.1175/jas3753.1

Goody, R. M., & Yung, Y. L. (1995). *Atmospheric radiation: Theoretical basis*. Oxford University Press.

Held, I. M., & Hou, A. Y. (1980). Nonlinear axially symmetric circulations in a nearly inviscid atmosphere. *Journal of the Atmospheric Sciences*, *37*(3), 515–533. https://doi.org/10.1175/1520-0469(1980)037<0515:nascia>2.0.co;2

Hohenegger, C., & Stevens, B. (2016). Coupled radiative convective equilibrium simulations with explicit and parameterized convection. *Journal of Advances in Modeling Earth Systems*, *8*(3), 1468–1482. https://doi.org/10.1002/2016ms000666

Hopcroft, P. O., Valdes, P. J., & Ingram, W. (2021). Using the mid-Holocene "greening" of the Sahara to narrow acceptable ranges on climate model parameters. *Geophysical Research Letters*, *48*(6), e2020GL092043. https://doi.org/10.1029/2020gl092043

Isca development team. (2023). Isca. A framework for idealised global circulation modelling [Software]. Github. Retrieved from https://github.com/ExeClim/Isca

Jucker, M., & Gerber, E. P. (2017). Untangling the annual cycle of the tropical tropopause layer with an idealized moist model. *Journal of Climate*, *30*(18), 7339–7358. https://doi.org/10.1175/jcli-d-17-0127.1

Kang, S. M., Held, I. M., Frierson, D., & Zhao, M. (2008). The response of the ITCZ to extratropical thermal forcing: Idealized slab-ocean experiments with a GCM. *Journal of Climate*, *21*(14), 3521–3532. https://doi.org/10.1175/2007jcli2146.1

Kirtman, B. P., & Schneider, E. K. (2000). A spontaneously generated tropical atmospheric general circulation. *Journal of the Atmospheric Sciences*, *57*(13), 2080–2093. https://doi.org/10.1175/1520-0469(2000)057<2080:asgtag>2.0.co;2

Labonté, M.-P., & Merlis, T. M. (2023). Evaluation of changes in dry and wet precipitation extremes in warmer climates using a passive water vapor modelling approach. *Journal of Climate*, *36*(7), 2167–2182. https://doi.org/10.1175/jcli-d-22-0048.1

Lindzen, R. S., & Hou, A. V. (1988). Hadley circulations for zonally averaged heating centered off the equator. *Journal of the Atmospheric Sciences*, *45*(17), 2416–2427. https://doi.org/10.1175/1520-0469(1988)045<2416:hcfzah>2.0.co;2

Loeb, N. G., Doelling, D. R., Wang, H., Su, W., Nguyen, C., Corbett, J. G., et al. (2018). Clouds and the Earth's radiant energy system (CERES) energy balanced and filled (EBAF) top-of-atmosphere (TOA) edition-4.0 data product. *Journal of Climate*, *31*(2), 895–918. https://doi.org/10.1175/jcli-d-17-0208.1

MacDonald, C. G., & Ming, Y. (2022). Tropical intraseasonal variability response to zonally asymmetric forcing in an idealized moist GCM. *Journal of Climate*, *35*(24), 1–52. https://doi.org/10.1175/jcli-d-22-0344.1

Manabe, S. (1997). Early development in the study of greenhouse warming: The emergence of climate models. *Ambio*, 47–51.

Manabe, S., & Stouffer, R. J. (1988). Two stable equilibria of a coupled ocean-atmosphere model. *Journal of Climate*, *1*(9), 841–866. https://doi.org/10.1175/1520-0442(1988)001<0841:tseoac>2.0.co;2

Merlis, T. M., & Schneider, T. (2011). Changes in zonal surface temperature gradients and Walker circulations in a wide range of climates. *Journal of Climate*, *24*(17), 4757–4768. https://doi.org/10.1175/2011jcli4042.1

Merlis, T. M., Schneider, T., Bordoni, S., & Eisenman, I. (2013a). Hadley circulation response to orbital precession. Part I: Aquaplanets. *Journal of Climate*, *26*(3), 740–753. https://doi.org/10.1175/jcli-d-11-00716.1

Merlis, T. M., Schneider, T., Bordoni, S., & Eisenman, I. (2013b). Hadley circulation response to orbital precession. Part II: Subtropical continent. *Journal of Climate*, *26*(3), 754–771. https://doi.org/10.1175/jcli-d-12-00149.1

Mlawer, E. J., Taubman, S. J., Brown, P. D., Iacono, M. J., & Clough, S. A. (1997). Radiative transfer for inhomogeneous atmospheres: RRTM, a validated correlated-k model for the longwave. *Journal of Geophysical Research*, *102*(D14), 16663–16682. https://doi.org/10.1029/97jd00237

Privé, N. C., & Plumb, R. A. (2007). Monsoon dynamics with interactive forcing. Part I: Axisymmetric studies. *Journal of the Atmospheric Sciences*, *64*(5), 1417–1430. https://doi.org/10.1175/jas3916.1

Raymond, D. J. (2000). The Hadley circulation as a radiative–convective instability. *Journal of the Atmospheric Sciences*, *57*(9), 1286–1297. https://doi.org/10.1175/1520-0469(2000)057<1286:thcaar>2.0.co;2

Raymond, D. J., & Zeng, X. (2000). Instability and large-scale circulations in a two-column model of the tropical troposphere. *Quarterly Journal of the Royal Meteorological Society*, *126*(570), 3117–3135. https://doi.org/10.1002/qj.49712657007

Retsch, M.-H., Hohenegger, C., & Stevens, B. (2017). Vertical resolution refinement in an aqua-planet and its effect on the ITCZ. *Journal of Advances in Modeling Earth Systems*, *9*(6), 2425–2436. https://doi.org/10.1002/2017ms001010

Rios-Berrios, R., Bryan, G. H., Medeiros, B., Judt, F., & Wang, W. (2022). Differences in tropical rainfall in aquaplanet simulations with resolved or parameterized deep convection. *Journal of Advances in Modeling Earth Systems*, *14*(5), e2021MS002902. https://doi.org/10.1029/2021ms002902

Schneider, T., Bischoff, T., & Haug, G. H. (2014). Migrations and dynamics of the intertropical convergence zone. *Nature*, *513*(7516), 45–53. https://doi.org/10.1038/nature13636

Singh, M. S. (2019). Limits on the extent of the solsticial Hadley cell: The role of planetary rotation. *Journal of the Atmospheric Sciences*, *76*(7), 1989–2004. https://doi.org/10.1175/jas-d-18-0341.1

Sobel, A. H., Bellon, G., & Bacmeister, J. (2007). Multiple equilibria in a single-column model of the tropical atmosphere. *Geophysical Research Letters*, *34*(22), L22804. https://doi.org/10.1029/2007gl031320

Vallis, G. K., Colyer, G., Geen, R., Gerber, E., Jucker, M., Maher, P., et al. (2018). Isca, v1. 0: A framework for the global modelling of the atmospheres of Earth and other planets at varying levels of complexity. *Geoscientific Model Development*, *11*(3), 843–859. https://doi.org/10.5194/gmd-11-843-2018

Voigt, A., & Marotzke, J. (2010). The transition from the present-day climate to a modern Snowball Earth. *Climate Dynamics*, *35*(5), 887–905. https://doi.org/10.1007/s00382-009-0633-5

Waliser, D. E., & Somerville, R. C. (1994). Preferred latitudes of the intertropical convergence zone. *Journal of the Atmospheric Sciences*, *51*(12), 1619–1639. https://doi.org/10.1175/1520-0469(1994)051<1619:plotic>2.0.co;2

Williamson, D. L., & Olson, J. G. (2003). Dependence of aqua-planet simulations on time step. *Quarterly Journal of the Royal Meteorological Society*, *129*(591), 2049–2064. https://doi.org/10.1256/qj.02.62

Wing, A. A., Emanuel, K., Holloway, C. E., & Muller, C. (2017). Convective self-aggregation in numerical simulations: A review. *Surveys in Geophysics*, *38*(6), 1173–1197. https://doi.org/10.1007/s10712-017-9408-4

Zurita-Gotor, P. (2023). Data files for the manuscript "Non-uniqueness in ITCZ latitude due to radiation-circulation coupling in an idealized GCM" [Dataset]. Zenodo. https://doi.org/10.5281/zenodo.7789502